HYDROGEN SUPERSATURATIONS IN THE NORTH AND SOUTH ATLANTIC – A POSSIBLE INDICATOR OF NITROGEN FIXATION

by

Michael John Fraser

Submitted in partial fulfilment of the requirements

for the degree of Master of Science

at

Dalhousie University

Halifax, Nova Scotia

September 2012

© Copyright by Michael John Fraser, 2012

DALHOUSIE UNIVERSITY

Department of Oceanography

The undersigned hereby certify that they have read and recommend to the Faculty of Graduate Studies for acceptance a thesis entitled "HYDROGEN SUPERSATURATIONS IN THE NORTH AND SOUTH ATLANTIC – A POSSIBLE INDICATOR OF NITROGEN FIXATION" by Michael John Fraser in partial fulfilment of the requirements for the degree of Master of Science.

Dated: September 18, 2012

Supervisor: _____

Readers: _____

_____

_____

Departmental Representative: _____

DALHOUSIE UNIVERSITY

DATE: September 18, 2012

AUTHOR: Michael John Fraser

TITLE: HYDROGEN SUPERSATURATIONS IN THE NORTH AND SOUTH ATLANTIC – A POSSIBLE INDICATOR OF NITROGEN FIXATION

DEPARTMENT OR SCHOOL: Department of Oceanography

DEGREE: MSc CONVOCATION: May YEAR: 2013

Permission is herewith granted to Dalhousie University to circulate and to have copied for non-commercial purposes, at its discretion, the above title upon the request of individuals or institutions. I understand that my thesis will be electronically available to the public.

The author reserves other publication rights, and neither the thesis nor extensive extracts from it may be printed or otherwise reproduced without the author's written permission.

The author attests that permission has been obtained for the use of any copyrighted material appearing in the thesis (other than the brief excerpts requiring only proper acknowledgement in scholarly writing), and that all such use is clearly acknowledged.

_____

Signature of Author

DEDICATION PAGE

To my parents and Jenny

TABLE OF CONTENTS

LIST OF TABLES vii
LIST OF FIGURES viii
ABSTRACT x
LIST OF ABBREVIATIONS USED xi
ACKNOWLEDGEMENTS xii
CHAPTER 1 INTRODUCTION 1
1.1 Introduction 1
1.2 A brief review of nitrogenase-mediated nitrogen fixation 2
1.2.1 Nitrogen fixation 2
1.2.2 Nitrogenase 3
1.3 Methods of measuring nitrogen fixation 4
1.3.1 Acetylene reduction assay 5
1.3.2 $^{15}N_2$-tracer incubation 5
1.3.3 Geochemical-based nitrogen fixation estimates 6
1.4 Oceanic dissolved hydrogen measurements 7
1.4.1 Methods 7
1.4.2. Precautions against contamination 8
1.4.3. Negative sampling contamination 8
1.4.4. Historical measurements of dissolved hydrogen in the ocean 10
1.4.5. Laboratory studies of diazotroph hydrogen production 20
1.5 Hydrogenase 22
1.6 Photochemical production and diurnal variation of hydrogen concentrations in marine environments 23
1.7 Objectives of the present study 27
CHAPTER 2 METHODS 29
2.1 Introduction 29
2.2 Cruise track 29
2.3 Sample collection 30
2.4 Air samples 30
2.5 Equilibrator 31

2.6 Reducing gas analyser 31
2.7 Standards 32
2.8 Valve controller 33
2.9 Humidity 35
2.9.1 Efficiency of the Nafion tubes 36
2.10 Calculating seawater hydrogen concentrations 37
2.11 Flow rates 39
2.11.1 Laboratory flow rate calibration 40
2.11.2 Temperature effects on water flow rates 41
2.11.3 Water flow rates in the field 41
2.12 Temperature 45
2.13 Efficiency calculations 46
2.14 Blanks 47
2.15 Fluorescence measurements 47
CHAPTER 3 DATA PROCESSING 48
3.1 Gaps in the data 48
3.2 Contamination from the ship 49
3.3 Anomalous hydrogen peaks 55
CHAPTER 4 PRELIMINARY DISCUSSION OF RESULTS 58
4.1 Hydrogen concentrations along the AMT20 transect 58
4.2 Hydrogen as an indicator of nitrogen fixation rates 61
4.3 Distribution of nitrate and phosphate 65
4.4 Fluorescence and hydrogen concentrations 67
4.5 Wind speed and hydrogen concentrations 68
4.6 Sea surface temperature and hydrogen concentrations 71
4.7 Salinity and hydrogen concentrations 72
4.8 Directions for future work 73
BIBLIOGRAPHY 75
APPENDIX A 80
APPENDIX B 83

LIST OF TABLES

Table 1 Hydrogen concentrations at 2 stations in the South Atlantic…….pg 17

LIST OF FIGURES

Figure 1.1	Comparison of clean and contaminated water samples from Moore *et al*. (2009)……...……	pg 9
Figure 1.2	Vertical profile of hydrogen concentrations in the tropical North Atlantic from Herr & Barger (1978)……	pg 11
Figure 1.3	Vertical profile of hydrogen concentrations in the Norwegian Sea from Herr, Scranton & Barger (1981)…….....	pg 13
Figure 1.4	Surface hydrogen concentrations in the Norwegian Sea from Herr, Scranton & Barger (1981)…….…….....	pg 14
Figure 1.5	Hydrogen concentrations measured over a day-night cycle from Herr *et al.*(1984)…….....	pg 24
Figure 2.1	A map of the AMT20 cruise track……...	pg 29
Figure 2.2	A schematic of the air segmented continuous-flow equilibrator…….	pg 32
Figure 2.3	A schematic of the solenoid valve setup…….....	pg 34
Figure 2.4	Hydrogen peak areas measured with and without the Nafion tube in place…	pg 35
Figure 2.5a	The weight of water vapour trapped in drying tubes without a Nafion tube in place……..	pg 36
Figure 2.5b	The weight of water vapour trapped in drying tubes with a Nafion tube in place……	pg 36
Figure 2.6	Flow rates measured over a 27-hour period in the laboratory…….	pg 40
Figure 2.7a	Flow rates measured during the AMT20 cruise……...	pg 43
Figure 2.7b	Interpolated flow rates measured during the AMT20 cruise……...	pg 43
Figure 2.8	Flow rates measurements subsequent to a Tygon tube change……	pg 45
Figure 3.1	Hydrogen measurements made while approaching station……..	pgs 50-51
Figure 3.2	Hydrogen measurements made from samples taken from the surface to 10m	pg 52
Figure 3.3a	Cruise track of the *RRS James Cook* on 12 November 2010, showing the ship going through its own track……..	pg 54
Figure 3.3b	Hydrogen measurements made when the ship crossed its own track.....	pg 54
Figure 3.4a	Hydrogen concentrations with all underway measurements……	pg 57
Figure 3.4b	Underway hydrogen measurements, with anomalous measurements removed using a "running median" function……	pg 57

Figure 3.4c	Underway hydrogen measurements, with anomalous measurements removed using a " smoothing" function……	pg 57
Figure 4.1a	Hydrogen concentrations with anomalous measurements removed……	pg 60
Figure4.1b	Hydrogen saturation levels from underway measurements.....…..……	pg 60
Figure 4.2	Surface nitrogen fixation rates, integrated nitrogen fixation rates and surface *Trichodesmium* distributions for AMT17 from Moore *et al.* (2009a)…….	pg 62
Figure 4.3a	Hydrogen concentrations and nitrogen fixation rates from AMT20……	pg 64
Figure 4.3b	Hydrogen concentrations plotted against nitrogen fixation rates with weighted and unweighted linear regresisons……	pg 64
Figure 4.4a	Underway hydrogen concentrations with anomalous measurements removed……	pg 66
Figure 4.4b	Nitrate concentrations along the AMT20 transect, data from the World Ocean Atlas (up to 2009)…….	pg 66
Figure 4.4c	Phosphate concentrations along the AMT20 transect, data from the World Ocean Atlas (up to 2009)…….	pg 66
Figure 4.5	Fluorescence and hydrogen concentrations measured on AMT20….....	pg 67
Figure 4.6a	Wind speed and hydrogen concentrations measured on AMT20……	pg 69
Figure 4.6b	Wind speed and hydrogen concentrations measured between 6°N and 22°S on AMT20……	pg 69
Figure 4.6c	Wind speed plotted against hydrogen concentrations measured between 6°N and 22°S with a linear regression for wind speeds less than 15 m/s ……...	pg 70
Figure 4.6d	Wind speed plotted against hydrogen saturation levels measured between 6°N and 22°S with a linear regression for wind speeds less than 15 m/s……	pg 70
Figure 4.7	Sea surface temperature and hydrogen concentrations measured on AMT20	pg 71
Figure 4.8	Salinity and hydrogen concentrations measured on AMT20……...	pg 72

ABSTRACT

It has been demonstrated that nitrogen fixation is a source of hydrogen (H_2) to the ocean and therefore measurements of H_2 concentrations may be used as a possible indicator of nitrogen fixation (Moore, Punshon, Mahaffey, & Karl, 2009). However, the limited number and sparse distribution of measurements of dissolved hydrogen and nitrogen fixation rates made in the open ocean in the past have made it difficult to quantify the relationship between them. Toward this end, a new method of equilibrating seawater samples for H_2 measurement was employed along the 13,000 km Atlantic Meridional Transect (AMT20) from UK to Chile, allowing H_2 to be measured from underway samples every 3.5 minutes and thereby considerably increasing the number and resolution of H_2 measurements made in the open ocean. These high-resolution measurements reveal two regions with high H_2 concentrations, one in the North Atlantic and one in the South Atlantic.

LIST OF ABBREVIATIONS USED

AMT	Atlantic Meridional Transect
β	Bunsen coefficient
CDOM	chromophoric dissolved organic matter
CF	Calibration factor
Chl	chlorophyll
CTD	conductivity/ temperature/depth sensor
LD	Light-Dark
nmol	nanomole (10^{-9} mole)
NMHC	non-methane hydrocarbon
P^*	A measure of the depletion of phosphate relative to nitrate
pmol	picomole (10^{-12} mole)
ppb	parts per billion
ppm	parts per million
r_n	Redfield ratio
SST	sea surface temperature
Tg	teragram
VOC	volatile organic compound

ACKNOWLEDGEMENTS

I would like to thank my supervisor, Bob Moore, for providing clear advice, support and useful criticisms that greatly improved this work. I would also like to express gratitude to my other committee members, John Cullen, Markus Kienast and Stephen Punshon for their comments, improvements and advice.

I am forever grateful to my parents, Mike and Elaine, who are a constant source of support and encouragement, are my greatest advocates and are always on hand with sound advice. However, it is my girlfriend Jenny whom I owe the most gratitude. Not only for moving 3000 miles away from family and friends so that I could complete my thesis, but continuously pushing me to be better, supporting me through difficult times and making my time in Canada immeasurably more fun.

I wish to thank my friends among the Oceanography department's students, for help and advice in scientific fields, but also for the sociability and camaraderie. Particular mention goes to Candace, Will and Lindsay, without whom I may have completed my thesis earlier, but my knowledge of Canadian culture, sports and cribbage would be significantly diminished.

The author acknowledges financial support in the form of postgraduate scholarships from Dalhousie University. I would also like to thank the officers and crew of the *RRS James Cook* whose help and expertise aided the completion of this research.

CHAPTER 1 **INTRODUCTION**

1.1 Introduction

Hydrogen (H_2) is a trace gas in the atmosphere that is present with a mixing ratio of about 565 ppb in clean tropospheric conditions and about 800 ppb in urban environments (Novelli, et al., 1999). The estimated atmospheric turnover time of H_2 is 1.8-2.3 years (Simmonds, et al., 2000). Atmospheric hydrogen concentrations are increasing, with levels more than doubling from deduced pre-industrial concentrations (Khalil & Rasmussen, 1990), this increase is attributed to anthropogenic activity, including more burning of biomass and oxidation of methane and non-methane hydrocarbons. A 3-year time series indicates a yearly increase of 0.6±0.1% H_2 yr^{-1} (Novelli, Lang, A, Hurst, Myers, & Elkins, 1999). Another source of molecular hydrogen to the atmosphere is the photochemical oxidation of methane and non-methane hydrocarbons to formaldehyde and the subsequent photolysis releasing hydrogen and carbon monoxide (Constant, Poissant, & Villemur, 2009). Finally, and relevant to this study, hydrogen is known to be released as an obligate byproduct of nitrogen fixation (Constant, Poissant, & Villemur, 2009; Moore, Punshon, Mahaffey, & Karl, 2009; Ogo, Kure, Nakai, Watanabe, & Fukuzumi, 2004). The main sinks of tropospheric hydrogen are microbial soil consumption and oxidation by hydroxyl radicals (Constant, Poissant, & Villemur, 2009).

In the atmosphere, natural and anthropogenic non-methane hydrocarbons (NMHC), a group of volatile organic compounds (VOC), are thought to be sources of H_2 after photo-degradation (Constant, Poissant, & Villemur, 2009). Examples include ethylene and terpenes that photo-dissociate producing secondary organic aerosols such as formaldehyde, which may further dissociate to H_2. Vehicle emissions are the major source of NMHCs in urban areas, with vegetation the primary emitter in rural areas. Hydrogen concentrations in the atmosphere have

increased due to its use in industry, particularly ammonia production, petroleum refining and the production of pharmaceuticals (Constant, Poissant, & Villemur, 2009).

The ocean is believed to be a net source of hydrogen to the atmosphere (Schmidt, 1974). In the surface ocean dissolved hydrogen is found supersaturated in the low latitude regions, but despite research into the mechanisms for this common feature it is still not fully understood (Herr, Frank, Leone, & Kennicutt, 1984). The comparatively few studies (Punshon, Moore, & Xie, 2007; Herr, Scranton, & Barger, 1981) in high latitude regions show lower supersaturation and, in some areas, undersaturated waters. One biological pathway for hydrogen to enter the ocean is via nitrogen fixation (Constant, Poissant, & Villemur, 2009) and, from the commonly-cited stoichiometry of nitrogen fixation, a 1:1 molar ratio of N_2 fixed to H_2 released is expected.

1.2 A brief review of nitrogenase-mediated nitrogen fixation

1.2.1 Nitrogen fixation

In some regions of the ocean, the availability of nitrogen limits productivity; the reduction of ubiquitous dinitrogen (N_2) gas to biologically-available ammonium is believed to relieve this nutrient limitation (Zehr, 2011). Biological nitrogen fixation is performed by diazotrophic cyanobacteria which use the resulting ammonia to synthesize amino acids and other nitrogen-containing biomolecules. Three major groups of diazotrophs have been identified in the open ocean: (i) the filamentous non-heterocyst-forming *Trichodesmium* (heterocysts are specialized cells that spatially separate oxygen-sensitive N_2 fixation from oxygen-evolving photosynthesis), (ii) the filamentous heterocyst-forming symbionts, and (iii) unicellular cyanobacteria. Estimates of global oceanic N_2 fixation from a number of sources are not well constrained and range from 5 – 200 Tg N yr^{-1} (Gruber & Sarmiento, 1997). These uncertainties may be due to poor spatial

coverage of estimates of N_2 fixation rates, errors in the measurements and the assumptions that must be made to scale up global estimates.

Most diazotrophs photosynthesize and therefore produce oxygen (Zehr, 2011). Nitrogenase, the enzyme that catalyzes N_2 fixation, is oxygen sensitive so some non-heterocyst-forming diazotrophs will temporally or spatially separate photosynthesis and N_2 fixation, and fix N_2 at night. Laboratory experiments using cultures of marine cyanobacteria have shown clear diurnal cycles in H_2 (Wilson, et al., 2010b; Simmonds, et al., 2000).

1.2.2 Nitrogenase

The enzyme responsible for catalyzing the biological reduction of dinitrogen gas is nitrogenase (Burgess & Lowe, 1996). This enzyme consists of two proteins, a Fe-protein and a MoFe-protein. The Fe-protein is reduced by ferredoxin, a strong reductant that mediates the transfer of electrons. When photosynthesis and N_2 fixation temporally overlap, electrons are supplied from the photolysis of water, but electrons may also be supplied from the uptake and subsequent oxidation of H_2 (Wilson, Kolber, Tozzi, Zehr, & Karl, 2012). When N_2 fixation and photosynthesis are temporally separated, electrons are supplied from the conversion of ATP to ADP in addition to carbohydrate respiration. The MoFe-protein is subsequently reduced by the supply of electrons from the Fe-protein. This transfer of electrons occurs in such a way that the MoFe-protein is able to reduce another substrate (such as nitrogen). The MoFe-protein contains the active site (on the MoFe cofactor) where nitrogen is reduced (Hoffman, Dean, & Seefeldt, 2009). The MoFe-protein also contains a P cluster, where it is believed that electrons are passed one at a time from the Fe-protein to the MoFe cofactor. After 8 Fe-protein cycles, in each of which one electron is transferred, N_2 is reduced to two NH_3 molecules and a molecule of H_2 is released (Burgess & Lowe, 1996). Ammonia is then assimilated by the organism through

enzymatic action to nitrogenous compounds required in the cell (Nagatani, Shimizu, & Valentine, 1971).

It is known that nitrogenase-mediated nitrogen fixation reduces protons and the reaction is described in section 1.3.1 (equation 3). However, it has long been unclear whether H^+ reduction represents a leakage of electrons from an oxidized site of the enzyme, or H_2 evolution is an essential part of the mechanismof N_2 reduction. In the first case a 1:1 ratio of H_2 evolution to N_2 fixation would not be demanded, while in the second, it would (Burgess & Lowe, 1996).

It is believed that protons are reduced at the active site on the FeMo cofactor. The reason why protons are reduced to H_2 is not entirely understood, but it has been suggested that hydrogen is eliminated from two metal hydride species (a hydrogen atom bound to a metal) leaving an electron-rich metal complex to which N_2 can bind (Ogo, Kure, Nakai, Watanabe, & Fukuzumi, 2004). This mechanism, therefore, suggests an obligatory one H_2 released per one N_2 reduced.

Some studies have inferred varying ratios of H_2 release to N_2 reduced. It was demonstrated by Rivera-Ortiz &Burris (1975) that 0.56 and 0.9 H_2 were evolved per N_2 reduced by extrapolating to an infinite partial pressure of nitrogen. However, in one experiment in which H_2 production and N_2 reduction by nitrogenase were measured under a partial pressure of nitrogen of 50 atmospheres, the ratio of H_2 produced to N_2 reduced was 1.13 ± 0.13 (± 1 standard deviation) (Simpson & Burris, 1984). Simpson and Burris (1984) suggest this is evidence that H_2 release is requisite in nitrogen fixation. In a review paper, Thornely and Lowe (1996) cite these two papers as evidence that H_2 release is obligatory in nitrogen fixation, but not necessarily in a 1:1 ratio.

1.3 Methods of measuring nitrogen fixation

Currently there are two key methods of measuring rates of nitrogen fixation, an acetylene (C_2H_2) reduction assay and $^{15}N_2$ incubations.

1.3.1 Acetylene reduction assay

Dilworth (1966) demonstrated that in the presence of acetylene, nitrogen fixation is inhibited. Furthermore, it was concluded that nitrogenase catalyzes the reduction of acetylene to ethylene. This process is used as an assay for nitrogen fixation. From the stoichiometry (equations 1 and 2), the ratio of N_2 fixed to ethylene produced is 3:1. However, this ratio has been shown to vary considerably, e.g. Scranton *et al.* (1987) reported ratios ranging from 3.3:1 to >50:1 for *Trichodesmium thiebautii* alone. So while the method has the advantage of being relatively simple to implement, this uncertainty in the value of the conversion factor leads to equivalent uncertainty in the calculated nitrogen fixation rate.

$$N_2 + 6H^+ + 6e^- \rightarrow 2NH_3$$

Equation 1.

$$3C_2H_2 + 6H^+ + 6e^- \rightarrow 3C_2H_4$$

Equation 2.

$$N_2 + 8H^+ + 16ATP + 8e^{-1} \rightarrow 2NH_3 + H_2 + 16ADP + 16Pi$$

Equation 3.

1.3.2 $^{15}N_2$-tracer incubation

Unlike the acetylene reduction assay, $^{15}N_2$ fixation gives a more unambiguous measure of the reduction of dinitrogen gas (Mohr *et al.,* 2010). A bubble of $^{15}N_2$ gas is injected directly into the discrete sample, which is then incubated for a period of time, typically 24 hours. After incubation, N_2 fixation rates are obtained from the measured incorporation of ^{15}N into particulate organic nitrogen (PON). Mohr *et al.* have suggested however, that this method may be underestimating rates of nitrogen fixation. They show that the injected bubble does not rapidly equilibrate with the water, with only 50% isotopic equilibration after 8 hours incubation, rising to

75% after 24 hours. A second experiment showed that spiking cultures of *Crocosphaera watsonii* with $^{15}N_2$-enriched artificial seawater, which was believed to be 100% equilibrated, yields 60% higher N_2 fixation rates than injecting $^{15}N_2$ gas directly. The authors suggest that this underestimation may explain, to some degree, the discrepancy between estimates of global N_2 fixation (adding biologically active nitrogen to the ocean) and denitrification (removing it).

1.3.3 Geochemical-based nitrogen fixation estimates

Acetylene reduction assays and $^{15}N_2$-tracer incubations only allow discrete measurements to be made; therefore identifying the spatial and temporal distribution of nitrogen fixation rates is difficult. Deutsch *et al.* (2007) describe a method of estimating nitrogen fixation rates through nitrate (NO_3^-) and phosphate (PO_4^{3-}) concentrations, of which there are many measurements (Gruber & Sarmiento, 1997). Because N_2-fixing organisms do not take up nitrogen and phosphorus in the typical 16:1 molar ratio (Redfield ratio, r_n), but in the extreme consume only PO_4^{3-}, the dissolved phosphate pool becomes progressively more depleted and NO_3^-:PO_4^{3-} ratios in the water increase above 16:1. One measure of the degree to which PO_4^{3-} is depleted relative to NO_3^- is $P^* = PO_4^{3-} - NO_3^- / r_n$ (mM).

Nitrogen fixation, in the theoretical model described by Deutsch *et al.* (2007), may therefore be observed as a decreasing P^* along the path of a water mass, and rates can be approximated from observed nutrient distributions, ocean circulation, and mixing rates (determined from an ocean circulation model). At steady state, excess PO_4^{3-} that is brought to the surface from circulation and mixing of the upper ocean is taken up in excess of the Redfield stoichiometry by diazotrophs to bring NO_3^- and PO_4^{3-} back to the observed concentrations. The rate of nitrogen fixation can, therefore, be thought of as the rate that N must be fixed to compensate for the excess PO_4^{3-}. The Deutsch *et al.* model also accounts for the recycling of dissolved organic matter (DOM) in the surface ocean and the export of diazotrophic biomass with high N: P ratios.

1.4 Oceanic dissolved hydrogen measurements

1.4.1 Methods

Methods for determining hydrogen gas concentrations have changed little over time, with the reduction of mercury oxide (HgO) being the preferred method of detection (Seiler & Schmidt, 1974). This method optically detects the mercury (Hg) vapour liberated when hydrogen and other reducing gases reduce HgO. A molecular sieve column is used to separate the various reducing gases in the sample including H_2 and CO. The peak area is then compared to measurements of gas standards, determined in the same way as the sample, in order to calculate the concentration of hydrogen in the sample.

Because a gas sample is required for this method, it is necessary to extract H_2 from the seawater sample before analysis. How the dissolved gas is extracted, depends to some degree on the type of water sample obtained. Measurements made on discrete samples frequently involved the extraction of the dissolved hydrogen through a static vacuum method (Seiler & Schmidt, 1974) (Herr & Barger, 1978). The seawater sample is drawn into an evacuated (to 13 Pa) glass bulb with a septum and stopcock, where it rapidly out-gases, giving a gaseous sample that can be analyzed.

Setser *et al.* (1982) described a continuous flow equilibration method to extract a gaseous H_2 sample. A H_2-free gas stream was bubbled (at ~80 mL/min) into a continuous water sample that was collected from a towed fish. The water stream and bubbles moved through a glass coil in a water bath, where equilibration took place, before H_2 was separated and analyzed using the HgO reduction method.

Later, hydrogen gas samples were obtained using a headspace equilibrium method, initially developed for measurements of carbon monoxide in seawater (Bullister, Jr, N.L, & Schink, 1982;

Xie, et al., 2002). A syringe is used to sample an accurate volume of water, after which a known volume of H_2-free air is introduced as a headspace (Punshon, Moore, & Xie, 2007). The syringe is shaken for 3 minutes to ensure complete phase equilibration. The headspace is subsequently injected into the analyzer, and measured using the HgO reduction method.

1.4.2. Precautions against contamination

In a study of hydrogen concentrations in the Mediterranean Sea, Scranton *et al.* (1982) describe the extensive precautions that were taken to avoid potential contamination. Of particular concern was H_2 generation from the corrosion of sacrificial zinc anodes on the CTD rosette. To reduce this risk, the anodes were removed. Furthermore, corrosion of the metal frame of the CTD was limited by coating it with enamel paint. Lastly, the Niskin bottles on the CTD rosette were closed whilst still moving upward to get a sample that has had little contact with the rosette. The authors state that this procedure was imperative to obtaining a clean sample. It should be noted that even with these precautions 39% of H_2 replicate sample pairs were not within the analysis precision (8-10% or 1 nL/L).

Because ships are generally fitted with zinc anodes Setser *et al.* (1982), we were concerned that contamination could occur during the crossing of other ship's tracks. However, H_2 measurements made while the ship was moving in a tight circle, showed no variation from oceanic concentrations. They conclude therefore, that contamination from the ship's track or from other ships is unlikely.

1.4.3. Negative sampling contamination

Hydrogen measurements made from an underway sampling system showed that there was significant loss of H_2 in the plumbing of the system (Moore *et al.*, 2009), perhaps due to H_2 removal by a biofilm. Samples from the laboratory were compared with samples taken from close

to the intake of the ship's seawater supply. Water from the ship's intake had concentrations on average 3.5 times higher than water from the laboratory tap (see figure 1.1).

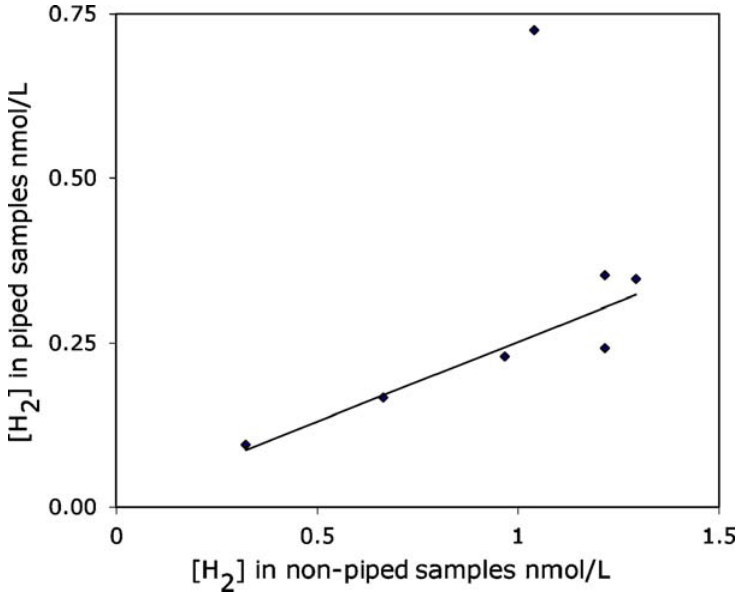

Figure 1.1. Plot of H_2 in water from the ship's contaminated supply ("piped" samples) plotted against values for samples that did not pass through the ship's plumbing. The regression line ($y=0.009+0.234x$; $r^2=0.86$) excludes the outlying data point. Reprinted from "The relationship between dissolved hydrogen and nitrogen fixation in ocean waters", Moore *et al*., 2009.

Moore *et al.* (2009) suggest that the removal of H_2 may be due to a biofilm forming in the plumbing of the ship's seawater supply. As the residence time of the water in the plumbing is estimated to be only a few minutes, the H_2 consumption is very rapid. Except perhaps for one outlier, the rate of H_2 uptake appears to be proportional to the H_2 concentration. Seemingly, the biofilm can take up H_2 as quickly as it is supplied for this range of H_2 concentrations. There is likely to be a point, however, when H_2 concentrations are high enough that the diffusive H_2 flux through the boundary layer to the microorganisms is more than enough to satisfy the utilization capacity of the organisms.

1.4.4. Historical measurements of dissolved hydrogen in the ocean

Early measurements of hydrogen made in the North Atlantic (~50°N to 40°N) and South Atlantic (~35°S to 65°S) found surface concentrations ranging from 0.8×10^{-5} to 5.0×10^{-5} mL/L (0.4 – 2.2 nmol/L) with average supersaturations of 300% (Seiler & Schmidt, 1974). Two methods were used to obtain both discrete and continuous samples. Discrete samples were collected to determine vertical profile concentrations; this involved a 5 L water sample being sucked into a 10 L evacuated flask where the sample rapidly dispersed into small droplets. With the rapid dispersal and the low pressure in the 10 L flask, equilibrium between the gaseous and liquid phases is quickly achieved. The 10 L flask was then filled to atmospheric pressure with air free of H_2 and CO, and then the whole gas sample was analyzed using the hot mercury oxide (HgO) technique. In the same paper a continuous sample was obtained from a continuous, downward-flowing seawater sample that was mixed with a H_2-free, upward flowing air at the same flow rate. Hydrogen equilibrated with the air and provided a gas sample that could be analyzed.

The 300% saturation levels are not solely explained by physical or chemical processes, and are probably an indication of biological activity (Seiler & Schmidt, 1974). Of the 14 hydrographic stations they sampled, there was little similarity between profiles and few corresponding features (dissolved hydrogen maxima and minima). However, the authors pay particular attention to a station in the Gulf of Cadiz, where a dissolved hydrogen subsurface maximum at ~500 m had a concentration of 23×10^{-5} mL/L (equivalent to 10.3 nmol/L), equating to a supersaturation factor of 24. The high concentrations were attributed to high nutrient loading leading to high biological productivity (including hydrogen-producing bacteria). The outflow of the denser (and more saline) Mediterranean into this area acts as a horizontal barrier, slowing the sedimentation of particles, leading to an accumulation of bacteria and nutrients at the boundary.

In a later study in the tropical North Atlantic, H_2 measurements at 15 hydrographic stations were made from the surface to 5000 m (Herr & Barger, 1978). Hydrogen concentrations in the mixed layer ranged from 9.8 to 73 nL H_2/L H_2O (0.44 - 3.26 nmol/L). Concentrations were highest (and supersaturated) in the surface ocean and mixed layer and decreased to equilibrium at greater depths. In the study by Herr and Barger (1978), H_2 concentrations were generally lower than those measured by Seiler and Schmidt (1974). Only 3% of all measurements made along the 4800 nautical-mile (8900 km) cruise track were greater than 300% supersaturation. There were cases of hydrogen subsurface maxima as shown at station 10 near the Cape Verde Islands (see figure 1.2). The subsurface maxima were found in the pycnocline, immediately below the mixed layer, perhaps a signal of biological hydrogen production or horizontal transport from advective processes (Scranton & Brewer, 1977).

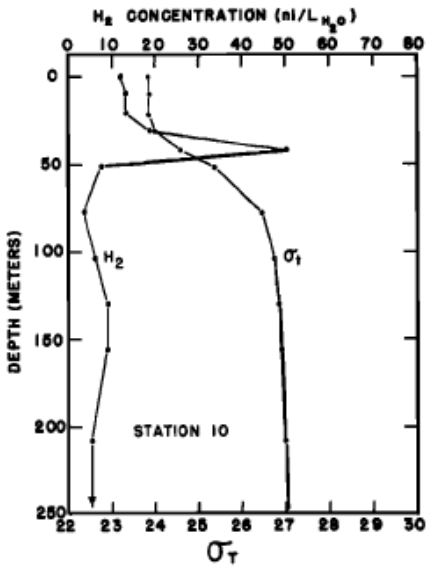

Figure 1.2. Vertical profile of H_2 concentration and σ_T at station 10. Reprinted from "Molecular hydrogen in the near-surface atmosphere and dissolved in waters of the Tropical North Atlantic," F. L. Herr and W. R. Barger, 1978. Sigma-t is the density of the water at the temperature and salinity of the sample.

A subsurface H_2 maximum reported at a station in the Gulf of Cadiz in Seiler and Schmidt's paper (1974) was not observed 4 years later in Herr and Barger's study (1978). This may be due to conditions no longer favouring bacterial production of hydrogen, analytical error or production being localized or short-term and thus missed in this cruise. Regardless, there is no evidence that the structure of the profile is permanent on yearly timescales.

Herr and Barger (1978) also took periodic near-surface atmospheric samples at the 15 hydrographic stations. Concentrations of hydrogen in the air samples ranged from more than 1.25 ppmv in the Straits of Gibraltar to ~0.62 ppmv away from anthropogenic influences. They reported an average atmospheric hydrogen concentration of 0.65 ppmv. This is slightly higher than air measurements of Seiler and Schmidt (1974) who found atmospheric H_2 concentrations of 0.56 ppmv.

In contrast to measurements made in tropical and sub-tropical regions, H_2 concentrations in the high latitude waters of the Norwegian Sea were below saturation (Herr, Scranton, & Barger, 1981). Samples were undersaturated from the surface to 3000 m, but some vertical profiles showed subsurface H_2 minima (see figure 1.3). The uniformity of low H_2 concentrations throughout the water column, even with a H_2 flux from the atmosphere to the mixed layer, implied a near-surface sink. Since the calculated exchange time of the upper 300 m of the water column with the atmosphere is 3 days to 1 month, the H_2 sink must persist for this time to maintain the observed undersaturation. The authors suggest that this sink may be chemolithotrophic H_2 oxidizing bacteria.

To establish the extent of surface variability of H_2 concentrations in the Norwegian Sea, Herr *et al.* (1981) sampled 3 areas in a grid pattern, with a station spacing of 4 km. Each station was re-sampled 6 days later. In one sample area, average H_2 concentrations varied very little, only changing from 0.27 ± 0.02 nmol L^{-1} to 0.30 ± 0.03 nmol L^{-1}. Although differences between

neighbouring stations within each sampling area were usually relatively small (rarely >0.09 nmol L^{-1}), variability in H_2 was observed in the region. This variability was observed in patches (see figure 1.4) and was attributed to biological activity. In this region, a spring bloom occurred just before sampling and the patchiness is believed to be a chemical signature of this bloom.

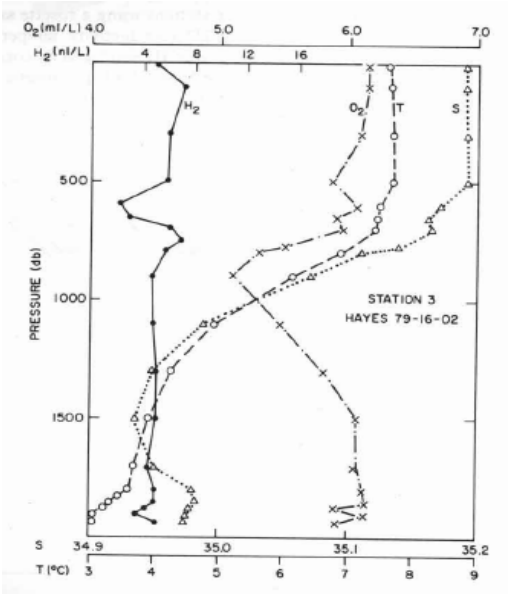

Figure 1.3. Vertical profiles showing subsurface H_2 minima in the Norwegian Sea. Reprinted from "Dissolved hydrogen in the Norwegian Sea: Mesoscale surface variability and deep-water distribution," by Herr, Scranton and Barger (1981).

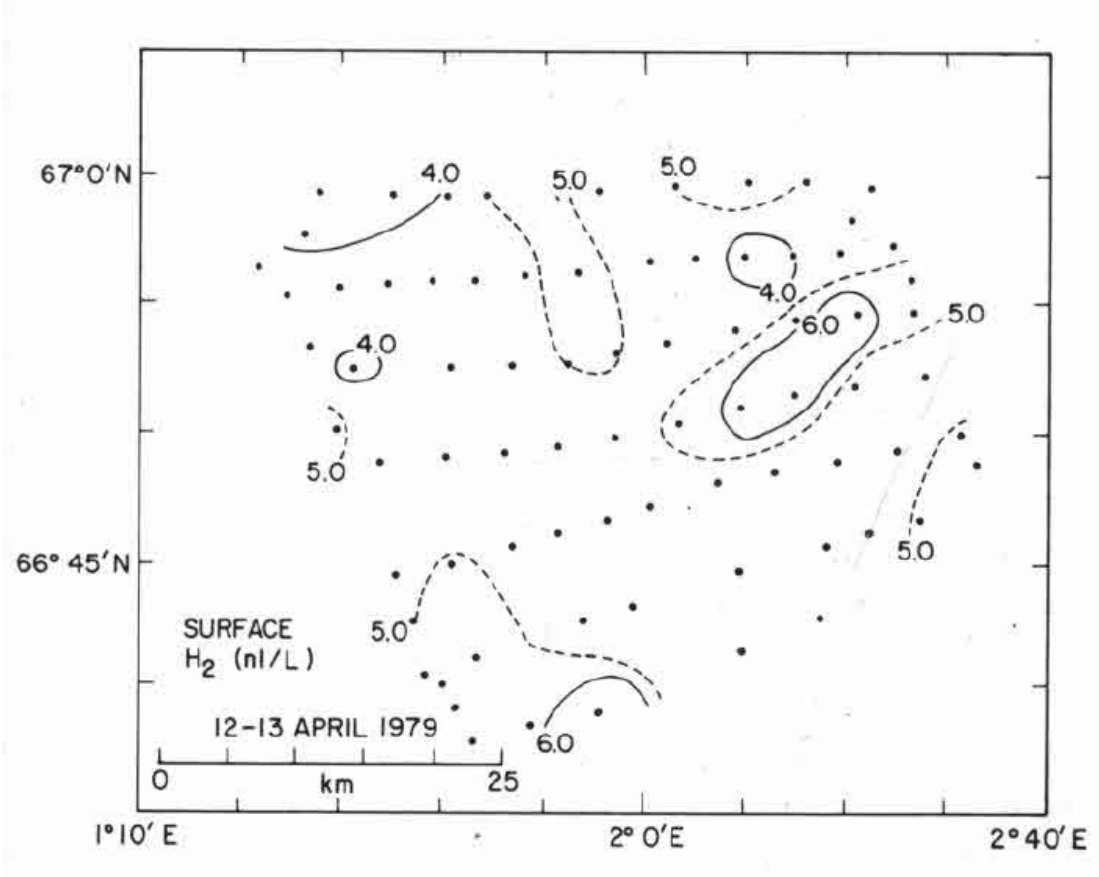

Figure 1. 4. Surface-sampled dissolved H_2 measured over two days. Samples were taken in a similar area 3 days later showing comparable concentrations and patchiness. Reprinted from "Dissolved hydrogen in the Norwegian Sea: Mesoscale surface variability and deep-water distribution" by Herr, Scranton and Barger (1981).

Vertical profiles of dissolved H_2 measurements made in the Mediterranean Sea showed supersaturations of 200-400% in the mixed layer, and undersaturations (or values close to the calculated atmospheric equilibrium) below the mixed layer (Scranton, Jones, & Herr, 1982). However, as in previous studies, there were occurrences of subsurface H_2 maxima. At two stations in the Alboran Sea, subsurface maxima were observed coinciding with the boundary of incoming North Atlantic Water and outgoing Mediterranean water. The top of this feature also coincided with a turbidity maximum as measured with a nephelometer, likely a result of sinking

particles accumulating at the density discontinuity between the two water masses. Therefore, the subsurface maximum may be a result of biological activity at this boundary.

Hydrogen concentrations off the coast of Baja California, in the California Current system, measured using a continuous-flow equilibrator, were generally steady, ranging from 0.3 – 0.6 nM (Setser, Bullister, Frank, Guinasso Jr, & Schink, 1982). The ship passed through 4 temperature-defined water masses. When the ship crossed a thermal boundary between waters cooler than 20.3°C and waters in the range 20.3 – 21.3°C, H_2 concentrations increased to a maximum of 3.7 nM. When the ship came within 100 km of the coast, it crossed another boundary but this time into warmer waters (>22.1°C). Here there were huge variations in the H_2 concentrations, reaching a maximum of 21.4 nM. These concentrations are among the highest that have been recorded in the literature. In the warm water mass, H_2 concentrations and chlorophyll fluorescence were strongly correlated (r=0.97), but this correlation was not observed in other water masses. Setser *et al.* (1982) suggest that the distinct changes in H_2 distribution may be a result of different biota in each water mass.

Anaerobic organisms are known to produce and consume H_2 (Nandi & Sengupta, 1998). Scranton *et al.* (1984) made H_2 measurements in two different anaerobic environments. The first was in Salt Pond, a shallow (5.5 m), seasonally anoxic basin in Falmouth, MA. During summer stratification, the water below 3-4 m becomes anoxic and a bloom of photosynthetic sulfur bacteria forms at the boundary. Hydrogen concentrations above the anoxic zone were at equilibrium with the atmosphere. Hydrogen concentrations in the anoxic zone increased with depth to a concentration 2-4 times atmospheric equilibrium.

The second site in this study was the Cariaco Trench, a permanent and comparatively more stable marine anoxic environment. The water here is oxic from the surface to 300 m. Hydrogen data for the Cariaco Trench show a 30% supersaturation in the surface waters that quickly decreases with

depth. At the oxic/anoxic interface hydrogen concentrations increase to values 2-4 times those just above the interface. Scranton *et al.* (1984) suggest that this may be due to anaerobic fermentation processes occurring at the boundary. In comparison, the Salt Pond has a larger flux of organic material, hydrogen concentrations an order of magnitude higher than in the Cariaco Trench, and higher concentrations of bacteria.

Continuous measurements of dissolved H_2 in the South Atlantic made by Herr *et al.* (1984) showed some correlation with irradiance along a 900 km section, suggesting a diurnal cycle in H_2 production or consumption. The diurnal cycle observed in this study is discussed in more detail in section 1.6. These authors report depth profiles taken at stations 8 and 9 (Table 1). At both stations, H_2 concentrations in the mixed layer were higher than atmospheric equilibrium but the excess H_2 did not extend to the base of the euphotic zone. At station 8, the highest H_2 concentrations were at the surface of the mixed layer, suggesting that surface production outcompeted mixing. Within the mixed layer at station 9, the lower H_2 concentration at 15 m suggests that there was either rapid mixing throughout the mixed layer with H_2 consumption at 15 m, or there was slow mixing throughout the layer and the measurements at 30 m and 40 m show the previous day's H_2 accumulation.

Table 1 Hydrogen concentrations at 2 stations in the South Atlantic. Station 8 was sampled just before 1900h local time and station 9 was sampled after 0715h. Reprinted from "Diurnal variability of dissolved molecular hydrogen in the tropical South Atlantic Ocean" by Herr *et al.* 1984.

Table 1. Hydrogen profiles

Depth (m)	Sta. 8, 9 March 82 (1330Z) 14°59′S, 23°58′W H_2(nl l^{-1})	Sta. 9, 13 March 82 (1630Z) 12°33′S, 27°47′W H_2(nl l^{-1})
3	32.3	22.1
15	22.5	15.3
30	20.6	25.6
45	13.6	21.4
60	12.1	6.7
70	6.3	3.8

Shore-based incubations of the marine diazotroph *Oscillatoria thiebautii* (now *Trichodesmium*) showed significant production of hydrogen (Scranton, 1984). Rates of H_2 production by colonies of *Oscillatoria thiebautii*, collected using a 150 µm-mesh plankton net, ranged from 0.044 µmol m^{-2} d^{-1} to 0.038 µmol m^{-2} d^{-1} (assuming a uniform colony density and production rate over a 20 m mixed layer depth). She calculated that the measured hydrogen production rates could create surface supersaturations, but only if there were no loss processes. The waters near Bermuda however, were undersaturated with hydrogen.

Scranton (1984) showed that the waters near Bermuda were consistently undersaturated with H_2, suggesting that loss processes are acting at greater rates than biological production and flux from the atmosphere. She states that because the hydrogen concentrations at one station did not change over several days, lateral advection is likely to be an insignificant removal process. Biological consumption and diffusive loss to the thermocline are believed to be the key loss processes.

Scranton *et al.* (1987) tested whether variability of the ratio of acetylene reduction to N_2 fixation in colonies of *Oscillatoria thiebautii* was a result of sampling methodology rather than hydrogen

production. It had previously been demonstrated that disturbances of the *Oscillatoria thiebautii* colonies strongly decreased nitrogen fixation rates. In addition to this, nitrogen fixation rates varied in the presence of copper ions. To negate these problems colonies of *Oscillatoria thiebautii* were collected in trace metal clean conditions by a diver and transferred to argon-flushed vials.

Both acetylene reduction and $^{15}N_2$ fixation assays were performed on diver-collected colonies and with colonies collected with nets towed by the ship. Comparisons of both procedures show more variability between days than between *in situ* and ship incubations. The most dissimilar absolute rates of acetylene reduction of *in situ* and standard incubations were 1.24 ±0.71 nmol colony^{-1} h^{-1} and 1.05 ±0.58 nmol colony^{-1} h^{-1} respectively. Whereas over a 2 day period, rates changed from 1.79 ±0.59 nmol colony^{-1} h^{-1} to 0.94 ±0.24 nmol colony^{-1} h^{-1}.

Hydrogen production was also measured from diver-collected *Oscillatoria thiebautii* (now *Trichodesmium*) colonies (Scranton, Novelli, Michaels, Horrigan, & Carpenter, 1987). To account for any contamination from the ship, divers collected water samples for hydrogen determination too. Surface hydrogen concentrations reached 0.74 nM in the early part of the cruise, 2-3 times atmospheric equilibrium (the measured atmospheric H_2 concentration was lower than previous studies at only 0.42±0.02 ppm v), indicating excess production. However, after a storm, H_2 concentrations abruptly returned to the equilibrium value of 0.26 nM or lower. Rates of hydrogen production did vary with time of day and with water depth, suggesting that light availability may control hydrogen production. However, the authors of the study suggest that *Oscillatoria thiebautii* is not a major net source of H_2, with ratios of H_2 production to acetylene reduction of 0.002 to 0.014.

To assess whether it might be possible to use H_2 as an indicator of N_2 fixation, Moore *et al*. (2009) compared H_2 saturation with concurrent N_2 fixation rates that were determined by $^{15}N_2$

incubations along a transect from Suva, Fiji to Honolulu, Hawaii. In addition to samples taken from the ship's supply of seawater, samples were also taken from vertical profiles using a rosette of Niskin bottles.

As with previous measurements of H_2, contamination of samples was a concern and validation of H_2 concentrations was imperative in assessing whether there was any loss or production of H_2 from the sampling process (Moore, Punshon, Mahaffey, & Karl, 2009). Any potential contamination from corrosion from the rosette of Niskin bottles (in particular the sacrificial zinc anodes) was minimized by immediately closing the bottle at the desired depth on the upward profile. Furthermore, samples were collected from inside the ship near the seawater supply inlet (these are reported as non-piped) to compare with samples that were taken from the laboratory (piped) that had passed through the plumbing system. Comparisons of H_2 concentrations from the piped and non-piped samples suggested major loss within the ship's plumbing system, with the piped samples containing only 30% of that in the water entering the plumbing system. Although the residence time of the water in the plumbing was estimated to be only a few minutes, a bio-film was suggested as the potential source of the removal of H_2. Because the removal of H_2 was large enough that concentrations dropped below atmospheric saturation, cavitation was not the cause of this loss.

Hydrogen concentrations, corrected for the loss in the plumbing, varied from 0.3 to 12.6 nmol L^{-1} (Moore, Punshon, Mahaffey, & Karl, 2009). Hydrogen concentrations increased from 18°S to ~13°S where concentrations decreased abruptly to near atmospheric saturation. The precipitous drop in H_2 was seen in samples taken from the ship's seawater supply and from Niskin bottles, and was unlikely a result of a cessation of a contamination source.

The small number of data points for which both excess H_2 concentrations and N_2 fixation rates were available showed a strong correlation between nitrogen fixation rates (μmol N m^{-3} d^{-1}) and

the concentration of excess H_2 (nmol L^{-1}) (N_2 fixation = -0.15+1.73 $[H_2]_{excess}$, correlation coefficient, 0.96: n = 9) (Moore, Punshon, Mahaffey, & Karl, 2009). In the same study an attempt was made to determine whether a relationship was apparent between the production rate of H_2 and the rate of N_2 fixation. The estimation of the production rate of H_2 per unit volume of water was made by assuming that steady state existed between H_2 production and ventilation to the atmosphere. It was necessary to assume a steady wind speed and steady mixed layer depth at each station. The calculation gave a net rate of production of H_2 (because microbial uptake could not be assessed). The ratio of H_2 produced to N fixed varied from 0.09 to 0.59 suggesting that net H_2 production is not directly correlated with N_2 fixation. However, Moore *et al.* (2009) believe that the questionable assumption that the system is in steady-state means that the calculated H_2 production rates are uncertain and that firm conclusions cannot be drawn from these values.

1.4.5. Laboratory studies of diazotroph hydrogen production

To assess whether different diazotrophs produce varying amounts of H_2 (per N atom fixed), and to better understand the H_2 cycling, Wilson *et al.* (2010a) analyzed cultures of four diazotrophs over a 12:12 h light: dark cycle. Hydrogen production was measured in cultures of *Trichodesmium erythraeum, Cyanothece* sp. and two strains of *Crocosphaera watsonii* (WH8501 and WH0002), as was nitrogen fixation (determined by ethylene production). Because H_2 production and N_2 fixation ceased with the addition of ammonia to the cultures, it was believed that N_2 fixation was the source of H_2 production.

The highest rates of H_2 production and ethylene (C_2H_4) production were from *Trichodesmium erythrauem* cultures, reaching 3 nmol H_2 (μg chl *a*)$^{-1}$ h^{-1} and 32 nmol C_2H_4 (μg chl *a*)$^{-1}$ h^{-1} (Wilson, Foster, Zehr, & Karl, 2010a). Both hydrogen and ethylene production occurred during light periods and ceased with the onset of the dark period, which is consistent with reports of a

diel cycle of N_2 fixation by *T. erythraeum* (Punshon & Moore, 2008b). Of the four cultures, *Trichodesmium* was the only filamentous cyanobacterium.

Rates of H_2 and C_2H_4 production by *Cyanothece* sp. were 0.3-0.5 nmol H_2 (μg chl *a*)$^{-1}$ h^{-1} and 24 nmol C_2H_4 (μg chl *a*)$^{-1}$ h^{-1}. The maximum rates occurred during the dark period, with H_2 production lagging C_2H_4 production by 4 hours. Diazotrophs that fix nitrogen during dark periods, likely do so to temporally separate the incompatible processes of oxygen-producing photosynthesis and nitrogen fixation (Toepel, Welsh, Summerfield, Pakrasi, & Sherman, 2008).

The two strains of *Crocosphaera watsonii* also produced H_2 and C_2H_4 during the dark period of the experiment (Wilson, Foster, Zehr, & Karl, 2010a). Hydrogen production was a further order of magnitude lower than *Cyanothece* sp. for both strains with maximum rates of 0.028 and 0.018 nmol H_2 (μg chl *a*)$^{-1}$ h^{-1}. Ethylene production was similar to *Cyanothece* sp. however, at 24 and 16 nmol C_2H_4 (μg chl *a*)$^{-1}$ h^{-1}. Although this study normalized N_2 fixation rates to chlorophyll *a*, it complements the findings of Mahaffey *et al.* (2005) that demonstrated that filamentous cyanobacteria fix more N_2 per cell volume than unicellular cyanobacteria.

Stoichiometrically, the ratio of H_2 produced to N_2 fixed is 1:1, but in this study the ratio varied considerably between the diazotroph cultures, with *Trichodesmium erythraeum* producing the most H_2 per N_2 fixed (a ratio of 0.25-0.34). *Cyanothece* sp. had a ratio of 0.04-0.055 and the two strains of *Crocosphaera watsonii* having the lowest ratio of 0.003-0.004. The discrepancy from the 1:1 ratio was attributed to reassimilation of H_2, and the variation in the ratio of the four cultures is therefore due to varying efficiency of this reassimilation between species.

The significant contribution of nitrogen fixation by unicellular diazotrophs to the oligotrophic ocean has recently been established (Moisander *et al*., 2010). In a second study focusing on *Crocosphaera watsonii* (Wilson *et al.,* 2010b), measurements were made not only of H_2

production and N_2 fixation, but also O_2 production and consumption and photosynthetic efficiency in order to identify patterns in respiration, photosynthesis, N_2 fixation and H_2 production. Wilson *et al.* (2010b) concluded that *Crocosphaera watsonii* efficiently recycles H_2. They demonstrated that this organism fixes N_2 during the night, presumably to separate the interfering processes of O_2 production and N_2 fixation. An accumulation of O_2 during the light period was attributed to photosynthesis, and the subsequent decrease in O_2 concentrations during the dark period to respiration. The rate of O_2 utilisation doubles with the start of N_2 fixation, likely a result of increased energy demand. Despite H_2 and C_2H_4 production being limited to dark periods in a 12 hour light-dark (LD) cycle, under 24 hour light conditions H_2 and C_2H_4 production began at a similar time to production in the 12 hour LD regime but continued for 2-3 hours longer, suggesting that these processes are controlled by a circadian clock entrained to the light-dark cycle. When H_2 and C_2H_4 production was integrated over the 24 hour period, production rates were 93 and 88% of the 12 hour LD rates.

Wilson *et al*. (2010b) suggest that the efficient recycling of H_2 by *Crocosphaera watsonii* may be due to the temporal separation of photosynthesis and N_2 fixation. Because the pool of fixed carbon (required for N_2 fixation) cannot be replenished by photosynthesis during the dark period, there is greater demand for reassimilation of H_2 as an electron source. *Trichodesmium*, however, fixes N_2 during the light periods and is perhaps less dependent on reassimilation of H_2, which is shown in a higher net H_2 produced to N_2 fixed ratio (Wilson e*t al.,* 2010a).

1.5 Hydrogenase

Hydrogenases are enzymes that catalyze the evolution or consumption of molecular hydrogen (Bothe, Schmitz, Yates, & Newton, 2011). Reversible hydrogenases can function either in the evolution and consumption of H_2, whereas uptake hydrogenases function solely in the consumption of hydrogen. Most N_2-fixing cyanobacteria have a hydrogenase, but it may also be

present in non-diazotrophs. Bothe *et al.* (2011) suggest that the uptake of H_2 assists in regaining the ATP used by the bacterium during H_2 formation by nitrogenase, via respiration with H_2 as an electron donor.

1.6 Photochemical production and diurnal variation of hydrogen concentrations in marine environments

Variation in H_2 concentrations on a diel cycle could be indicative of biological production or consumption of hydrogen by organisms that are light sensitive (or photosynthesizing). Alternatively, variation of this kind may be a signal of photochemical production. Although there have been attempts to detect a diurnal cycle, there is little consensus on whether one exists. Seiler and Schmidt (1974) found no diurnal cycle in either the North or South Atlantic Oceans.

In one anoxic environment, however, the Salt Pond, nighttime H_2 concentrations were 2-3 times higher than daytime concentrations (Scranton, Novelli and Loud, 1984). Hydrogen uptake experiments were performed that showed that consumption of H_2 was independent of light intensity. Instead these authors suggest that photosynthetic sulphur bacteria produce H_2 during dark respiration and growth. The production of H_2 has been demonstrated by photoheterotrophs in the presence of reduced organic compounds during dark periods (Uffen, 1978).

However, measurements made in the tropical South Atlantic found the opposite diurnal cycle, with high daytime concentrations that declined during dark periods (Herr, Frank, Leone, & Kennicutt, 1984). In that study H_2 concentrations were strongly correlated with solar radiation (figure 1.5), with concentrations decreasing to atmospheric equilibrium during periods of darkness. The average rate of increase during daylight hours was 0.09 nM h^{-1}, and the rate of decrease during dark periods was 0.08 nM h^{-1}. The time between sunrise and the beginning of the increase in H_2 production varied from almost zero to 1 hour. Herr *et al.* (1984) suggest that the

most probable hydrogen removal mechanisms are loss to the atmosphere and mixing deeper into the water column. Advective removal processes are rejected, due to uniformity in hydrogen concentrations over the large areas covered by the ship. It should be noted that the diurnal variability was not observed over the entire cruise track, but in one 900 km section. The authors propose that a photochemical reaction with dissolved organic material may produce this diurnal cycle. In the lower atmosphere, formaldehyde (H_2CO) is photolyzed to give H_2 and CO; a similar reaction is proposed in the ocean but with higher aldehydes. These authors also suggested that hydrogen production might be a result of nitrogen fixation.

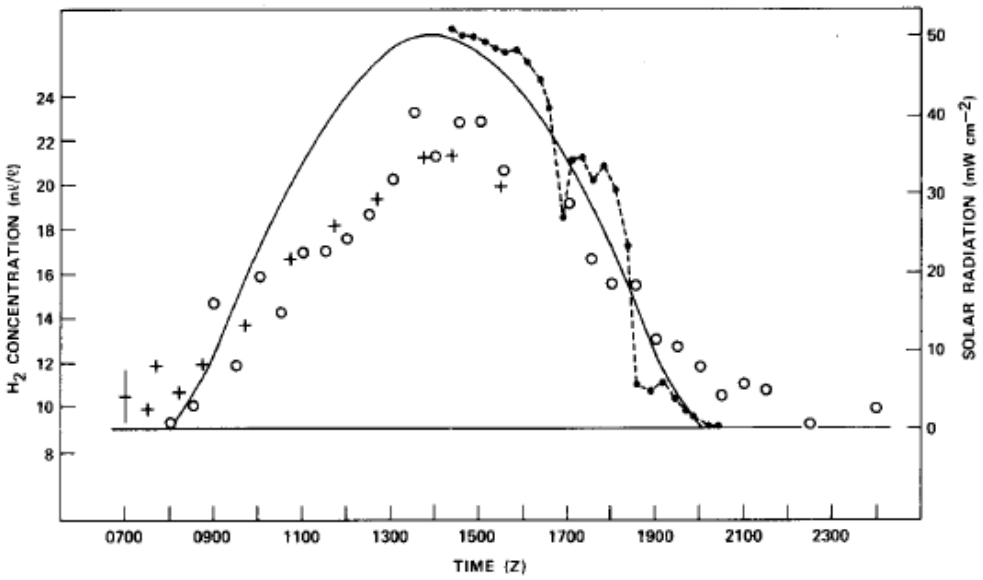

Figure 1. 5. Dissolved H_2 concentrations during daylight. O, 14 March 1982; +, 15 March 1982. The solid baseline is the air-sea exchange equilibrium concentration, 9.1nl l^{-1}. The dashed line is the measured global solar radiation for 14 March. The curve is the global solar radiation calculated from an ephemeris and Paltridge and Platt (1976). Sunrise on 14 March was at 0755 and on 15 March at 0810. Reprinted from "Diurnal variability of dissolved molecular hydrogen in the tropical South Atlantic Ocean" by Herr *et al.* (1984)

In 2007 Punshon *et al.* reported measured net loss rates of hydrogen at two locations in the coastal waters of eastern Canada. The first sample sites located in the St Lawerence Estuary,

Quebec, had net loss constants ranging from 0.29±0.03 d^{-1} in the lower estuary (areas with higher surface salinity) to 6.07 ±0.33 d^{-1} in areas with lower surface salinity. The second set of sample sites was located in two inlets in the eutrophic waters of Halifax Harbour, Nova Scotia. Net loss constants varied from 0.14 ±0.02 d^{-1} to 8.67 ±0.33 d^{-1} at one site (Bedford Basin), and from 0.36 ±0.02 d^{-1} to 2.67 ±0.32 d^{-1} at another site (Northwest Arm). Surface hydrogen concentrations in the Bedford Basin and the St. Lawrence Estuary ranged from ~0.05-2nM.

In the Northwest Arm, net loss rates exhibited a positive linear relationship with temperature. Net loss constants were calculated from dark-incubated water samples. A sample was divided into 4 subsamples, one that was left unfiltered, a second that was filtered through a Millipore 5 μm pore-size filter and the final set was filtered through a 0.2 μm pore-size membrane. Net H_2 loss constants were similar for the unfiltered and 5μm filtered samples, at 0.43 ± 0.06 d^{-1} and 0.39 ± 0.03 d^{-1} respectively. There was no significant net loss of H_2 in the ≤ 0.2 μm fraction, with a net loss constant of only 0.01 ± 0.04 d^{-1}.

In the same study some profiles made in Bedford Basin showed surface waters supersaturated with H_2 (118-257%), but this was only apparent on sunny days (Punshon, Moore, & Xie, 2007). Eight days later, under foggy conditions, the surface waters were undersaturated with H_2 (15%), suggesting that irradiance may be connected to a hydrogen production process. Alternatively, irradiance may be linked to an inhibition of hydrogen consumption. Comparison of unfiltered samples incubated in light and dark conditions showed lower net H_2 loss constants under light conditions; this is in agreement with observations made in the field.

The waters of the Gulf of St Lawrence and Bedford Basin were frequently undersaturated with H_2, with concentrations decreasing with depth (Punshon, Moore, & Xie, 2007). This is in agreement with the net loss rates measured in dark incubations. The authors suggest that that H_2 consumption may be prevalent in waters in the mid to high latitudes, as it is consistent with work

by Herr *et al.*(1984) who observed Arctic waters that were undersaturated with H_2. It is suggested that this loss is due to bacterial consumption, as the majority of H_2 loss occurred in the ≤5μm fraction and the unfiltered sample during the filtration experiment.

In a study to assess the possibility of photochemical H_2 production, water samples taken from freshwater and saltwater locations in Nova Scotia, Canada were filtered and then irradiated in natural and artificial sunlight (Punshon & Moore, 2008a). The authors suggest that H_2 may be produced from the photolysis marine aldehydes. In the atmosphere, formaldehyde and higher aldehydes are known to dissociate into H_2 and CO under ultraviolet radiation and it is postulated that similar reactions may occur in the marine environment. In aquatic regions, chromophoric dissolved organic matter (CDOM) is known to release these aldehydes by photodegradation, and it seems plausible therefore, that there may be a link between CDOM concentrations and H_2 production. Hydrogen production rates were measured in water taken from a lake with high CDOM levels, as well as pure water and 20% and 50% dilutions of lake water with pure water. Hydrogen production rates were linearly correlated with CDOM concentration ($r^2 = 0.997$, n = 4) (Punshon & Moore, 2008a). Furthermore, the irradiation of two carbonyl compounds (syringic acid and acetaldehyde), known to be formed from the degradation of humic substances and possibly a component of CDOM, led to an increase in H_2. However, because of the low concentrations of CDOM in oligotrophic waters, photochemical H_2 production is unlikely to explain the low-latitude H_2 supersaturation.

Punshon and Moore (2008b) suggested that nitrogen fixation is the most significant source of H_2 to low latitude regions, with *Trichodesmium erythraeum* producing 70% of the total 80 Tg N yr^{-1} to the oligotrophic ocean through nitrogen fixation. In laboratory experiments using cultures of *Trichodesmium*, H_2 production ranged from 0.06 to 0.71 nmol H_2 [μg Chl a^{-1}] h^{-1}. The 10-fold range in H_2 production may be attributed to differing growth stages of the culture, with the lowest

H_2 production rate from a culture in the early stages of growth and the highest rate from a culture in a later growth stage (Punshon & Moore, 2008b). Hydrogen production occurred 4-6 hours after the start of irradiation and peaked for 3 hours in the afternoon. Hydrogen concentrations measured at the beginning and end of a 12-hour dark period were much the same, suggesting hydrogen loss and production rates of zero or close to equilibrium. As with H_2 production, rates of nitrogen fixation varied considerably, from 0.12-4.71 nmol N_2 [μg Chl a^{-1}] h^{-1} (Punshon & Moore, 2008b). This may be due to the growth stage of the culture or a result of a depletion of inorganic combined nitrogen leading to increased nitrogen fixation rates.

In the same study, ratios of H_2 production to N_2 fixation for *Trichodesmium erythraeum* ranged from 0.15-0.48 and were an order of magnitude higher than those measured for *Trichodesmium thiebautii* colonies measured by Scranton *et al.* (1987), suggesting that perhaps *T. thiebautii* recycles H_2 more efficiently. The variability in the efficiency of H_2 recycling may be related to the growth stage of the organism, with an increase in the efficiency of older colonies. The depletion of H_2 may be a result of H_2-metabolizing bacteria that grow in the shelter of the tuft and puff *Trichodesmium* colonies. If H_2 measurements are to be used as indicators of N_2 fixation it will be necessary to know of any variability in the ratio of H_2 released to N_2 fixed.

1.7 Objectives of the present study

The review of the literature demonstrates relationships between N_2 fixation and H_2 production that are highly variable in ways that have yet to be well described. If robust correlations can be demonstrated between oceanic N_2 fixation rates and H_2 concentrations, then measurements of H_2 can be used as an indicator of N_2 fixation in future studies. Ideally, iron concentrations, implicated in the limitation of N_2 fixation (Falkowski, 1997), and many individual N_2 fixation

rates determined by $^{15}N_2$ incubations, would be compared with H_2 measurements to clarify the relationship between N_2 fixation and H_2 evolution. In this study however, no iron measurements were made and it was only possible to obtain 20 individual $^{15}N_2$ fixation rates, insufficient to draw any robust conclusions.

Therefore the primary focus of this study is to increase considerably the number of observations of hydrogen concentrations in the surface ocean. The majority of previous measurements have been made from discrete samples from stations kilometers apart. In this study a continuous flow equilibrator was used and measurements were made every 3 minutes along a 13,000 km transect.

CHAPTER 2 **METHODS**

2.1 Introduction

Dissolved H_2 concentrations were continuously measured in surface waters along a meridional transect in the North and South Atlantic and in vertical profiles. Due to the low concentrations (nM) of hydrogen in the surface ocean and possibilities of contamination, special precautions were made and sensitive equipment used.

2.2 Cruise track

In October to November of 2010, the *RRS James Cook* travelled from Southampton, England for Punta Arenas, Chile as part of the Atlantic Meridional Transect (AMT) program (see figure 2.1). The cruise track went from 49°N to 47°S and included mainly open ocean environments, although some measurements were made on the Patagonia shelf. Water temperatures ranged from 14.1 to 30.2°C and salinity from 32.02 to 37.75.

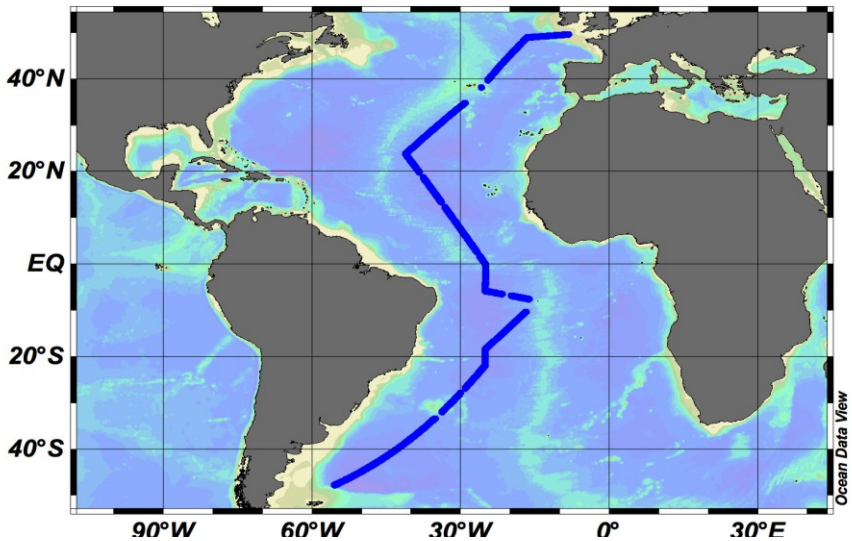

Figure 2.1. Map of the cruise track where hydrogen measurements were made during AMT20, October – November 2010.

2.3 Sample collection

Underway samples were pumped from a depth of ~7 m, through the ship's non-toxic system that fed taps in many of the ship's laboratories. From a laboratory tap, water flowed continuously at ~1 L min^{-1} to a reservoir. A peristaltic pump took a subsample from the reservoir to the equilibrator at approximately 14 mL min^{-1} (see Section 2.9). Corrosion of sacrificial zinc anodes, used to protect the hull of the ship, was a potential source of contamination. Two anodes forward of the ship's non-toxic intake had been removed while the ship was in dry dock to address this problem.

Profiles were sampled twice a day using a rosette of twelve 20 L Niskin bottles attached to a conductivity-temperature-depth (CTD) instrument. Samples were taken at pre-dawn and solar noon stations at intervals from the surface to maximum depths of 500 or 1000 m. For pre-dawn stations at the beginning of the cruise, a CTD with a titanium frame was used that did not require zinc anodes, which are a possible source of contamination. However, due to time and sampling constraints a stainless steel CTD was used for the remainder of the cruise that did have zinc anodes. 600 mL-sampling bottles were filled from the rosette and allowed to overflow by 2 volumes and until no air bubbles were in the sample. Samples were analysed in triplicate within 3 hours of collection. It should be noted that 5 measurements of each sample were made but the first and last values were normally discarded, as mixing of water from one sample to the next occurred.

2.4 Air samples

Air samples were collected in a 10 mL hypodermic syringe (Perfektum) from an oncoming wind at the ship's bow to minimize any influence from the ship. Two syringes were filled and the samples were typically measured within 20 minutes.

2.5 Equilibrator

An air-segmented, continuous flow equilibrator similar to that developed by Xie *et al.* (2001) was used to obtain a gaseous sample from seawater. A schematic of the equilibrator design is shown in figure 2.2. The procedure involves a continuous sample of seawater with a known flow rate being pumped through one port of a 3-way Delrin tee (custom made). At the same time, an air sample that is scrubbed of H_2 and CO by passage through a heated copper-manganese oxide combuster within the analyzer, flows at 2 mL min^{-1} through another port of the tee. The seawater sample, segmented by H_2-scrubbed air, moves through a vertical glass coil where phase equilibration takes place. The glass coil is enclosed in a water bath that buffers the variation in laboratory temperatures. The temperature of the water bath is automatically recorded on to the memory module of the valve controller. At the top of the glass coil a glass bubble separator allows the gas sample to be directed to the reducing gas analyser and the water sample to be discarded. Moisture was removed from the gas sample with a Nafion tube (see section 2.7).

2.6 Reducing gas analyser

Hydrogen measurements were made with a gas chromatograph that incorporated a reducing compound photometer (Peak Laboratories, USA). The equilibrated gas sample was introduced into the 1mL sample loop in the analyser. The reduction of heated mercuric oxide to mercury vapour by hydrogen is utilised to determine hydrogen concentrations, with the produced mercury vapour measured photometrically. The analyser is capable of measuring H_2 and CO simultaneously. Reducing gases are separated in a 2m long 1/8"column containing a Molesieve 13X that is heated to 105°C. The retention times for CO and H_2 were 110 seconds and 50 seconds respectively. For each measurement, a chromatogram was created from which a peak area was

calculated. When this peak area is compared to a peak area of a reference gas, it is possible to calculate the H_2 concentration of the sample.

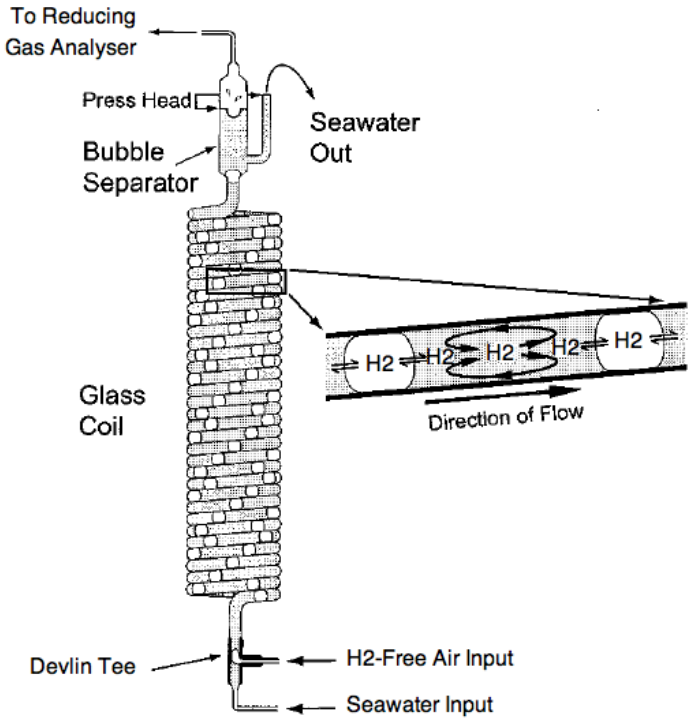

Figure 2.2. A schematic of the equilibrator and a diagram showing mixing in the glass coil. Adapted from "A simple automated continuous-flow-equilibration method for measuring carbon monoxide in seawater," by H. Xie, O. C. Zafiriou, W. Wang and C. D. Taylor

2.7 Standards

A gas standard with a known H_2 concentration (1.135 ppm) was used to calibrate and calculate the concentration of H_2 in the sample. Analysis of the gas standard produces a peak area. This peak area (or an average of many measurements) is divided by the known quantity of H_2 that has been measured (a function of the volume of the loop and the concentration of the gas standard) to give a calibration factor (CF).

CF (Peak area $nmol^{-1}$) = Peak area of reference gas/quantity of H_2 sampled

Equation 4

The sample peak area is then divided by this calibration factor to get the amount of H_2 (nmol) injected into the analyser, the concentration is obtained by dividing this by the volume of gas at STP injected into the analyser sample loop. This calibration factor is only valid when the response of the analyser is linear, which in this case is up to a water H_2 concentration of ~14 nmol L^{-1}(Moore & Punshon, 2007).

Commercially produced gas standards having the required composition and accuracy are unavailable, so a gas standard was made in the laboratory. A 30 L aluminium gas cylinder was completely evacuated and accurately weighed (± 0.1g). A volumetrically measured quantity of hydrogen at a measured temperature and pressure was then injected in a stream of air with a very low and measured H_2 concentration into the cylinder. The cylinder was then re-weighed to determine the mass of gas that was pumped into the cylinder. The concentration of the gas mixture was 1.135 ppm which was calculated from the concentration of H_2 in the diluting zero air and the volume of pure H_2 added.

2.8 Valve controller

Solenoid valves were used to alternately direct 3 different gas streams to the analyzer: the zero grade air, a reference standard and the sample. A combination of 3-way and 2-way valves were utilised to control the flows (figure 2.3). So that pressure does not build up, the sample gas is vented through a 3-way valve when not being analysed. The zero grade air is controlled by a 2-way valve, switching between on and off so that when it is not being measured it can be conserved.

Because of the complexity in producing the reference gases, conserving them was a priority. A combination of one 2-way valve and a 3-way valve was used to preserve the reference gas. When both valves were in the 'on' position, the reference gas could get through to the analyser. Prior to both being in the 'on' position, only the 2-way valve was switched on for 7 minutes to vent the tubing between the two valves. At all other times the two valves were in the 'off' position.

A 16-channel custom-designed valve controller was used to automatically switch between valves. A program controlled the position of each valve and when each switching occurred (see Appendix A). The program was loaded onto the valve controller using a USB drive, on which peak areas, temperatures and atmospheric pressures were stored.

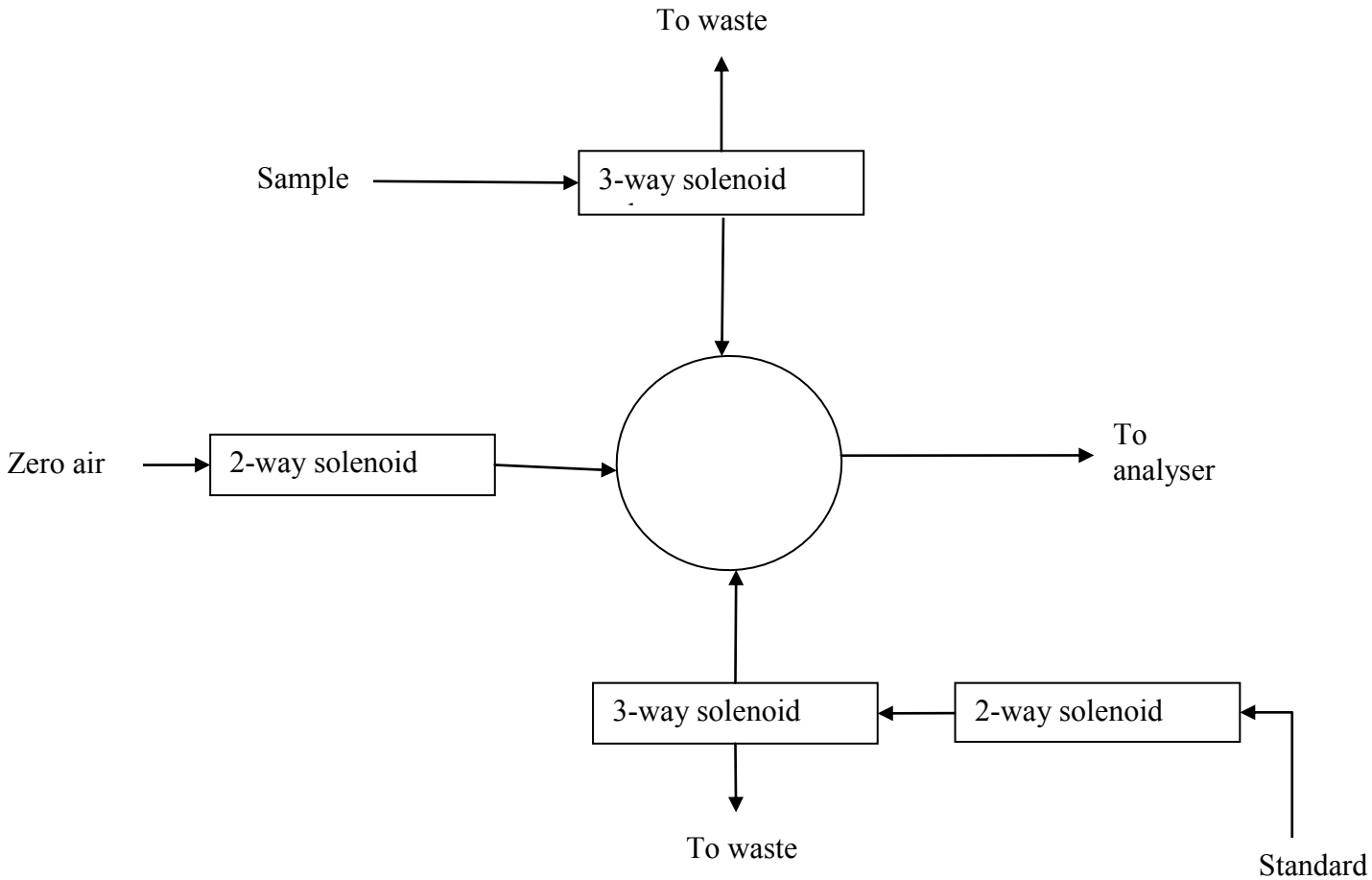

Figure 2.3. A schematic showing the arrangement of the solenoid valves

2.9 Humidity

A Nafion tube was used to reduce the water vapour content in the gas sample flowing from the equilibrator. If condensed water were to get into the reducing gas analyzer, considerable damage to the instrument as well as potential contamination from corrosion could occur. To assess the suitability of using Nafion tubes for the analyses, it was imperative to establish whether there would be any loss of hydrogen through the tubes.

This was done by measuring a gas sample of known hydrogen concentration greater than that found in the atmosphere, with and without the Nafion tube in place (figure 2.4). There is no statistical difference in peak areas between measurements made with and those made without the Nafion tubes, t (32) = 0.24, p = 0.81. The Nafion tube was installed between the bubble separator and the 3-way valve used to direct gas flow to the analyzer.

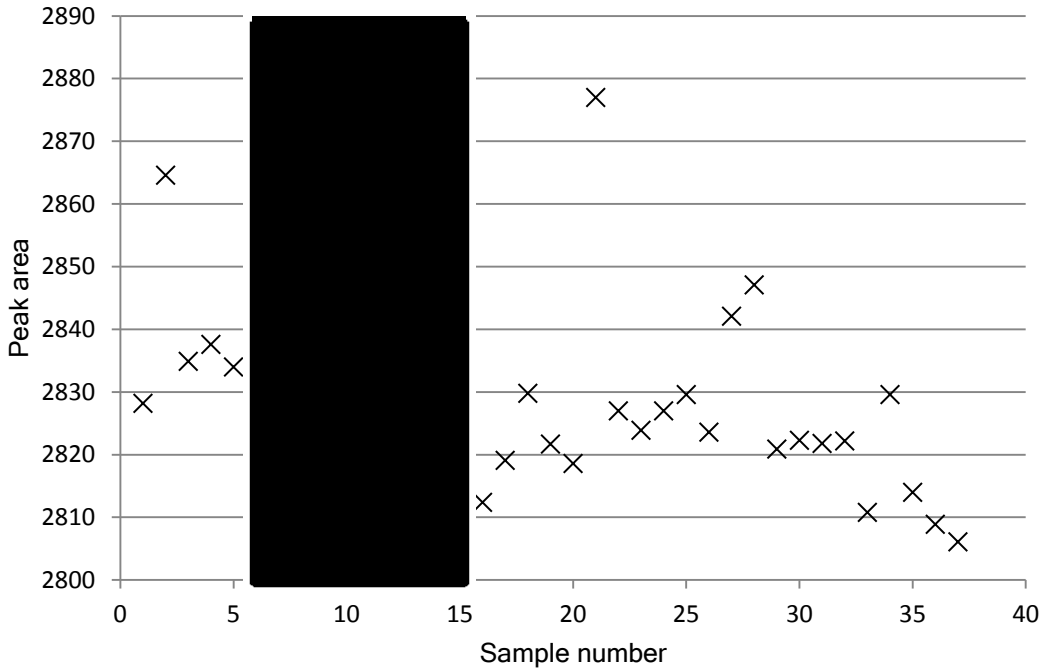

Figure 2.4. Peak areas measured from a gas of known concentration. The gas has been measured both with the Nafion tube in place (those in the shaded area) and without it.

2.9.1 Efficiency of the Nafion tubes

The effectiveness of the Nafion tube at removing water vapour from the gas stream flowing from the bubble separator was established by collecting the water vapour from the gas stream flowing from the bubble separator. The water was collected, both with and without the Nafion tube in place, in weighed drying tubes filled with magnesium perchlorate that were subsequently re-weighed after a period of time. The water sample had a temperature of ~25°C.

a

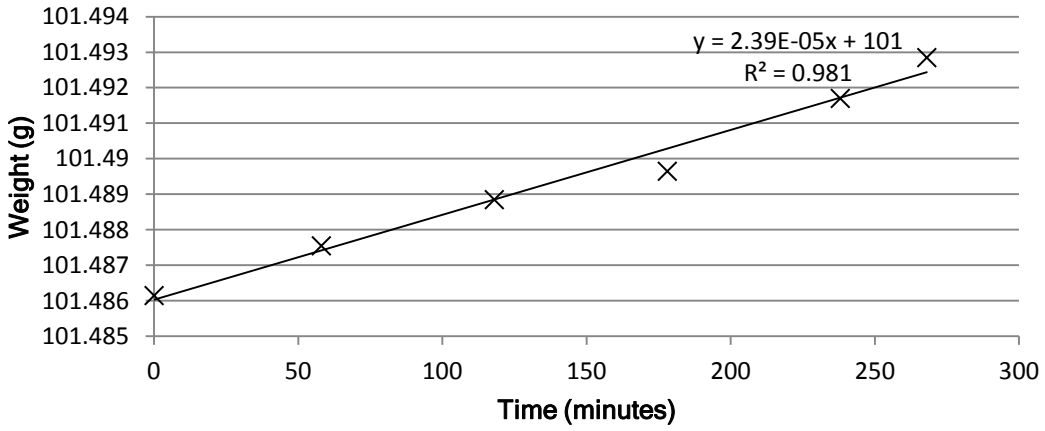

b

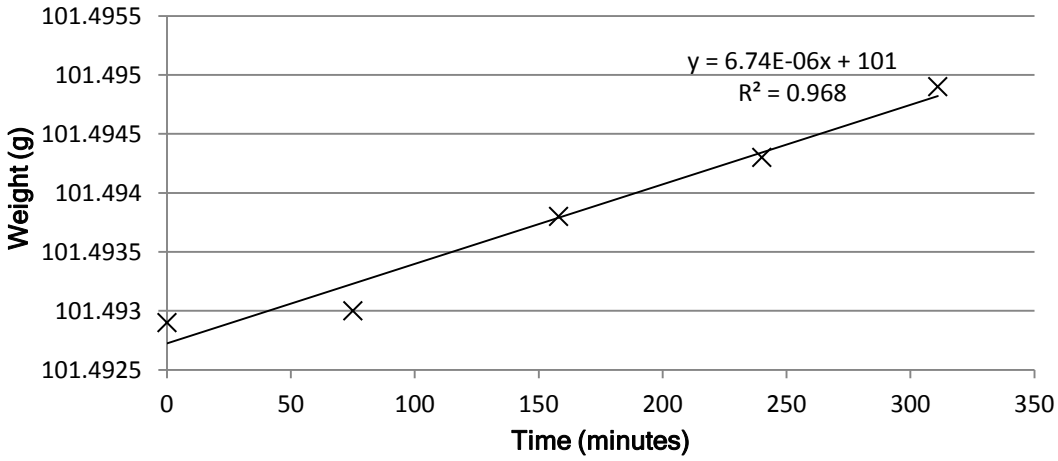

Figure 2.5a and b. The weight of a drying tube filled with magnesium perchlorate as a function of time. The increase in weight is attributed to the removal of water vapour from a gas sample passed through the drying tube. **a**, No Nafion tube is in place to remove water vapour. **b**, a Nafion tube is in place to remove water vapour.

The linear relationship shown in figure 2.5 suggests a constant rate of water vapour trapping in the drying tube when there is no Nafion tube in place. The average rate of water removal was measured at 2.5 x 10^{-5} g/min (cf. based on the water vapour pressure at 25 °C it would be calculated that the supply of water vapour is 2.3 x 10^{-5} g/min). With the Nafion tube in place (see figure 2.5b) there was also a linear increase in the weight of water trapped, showing a steady rate in the supply of water vapour, but the average rate of water vapour trapping was only 6.4 x 10^{-6} g/min, a factor of 4 smaller than without the Nafion tube. From the measurements made in this experiment it can be determined that 74% of the water vapour supplied from the equilibrator was removed by the Nafion tube.

$$\text{Percent removal of water by Nafion tube} = \frac{\text{rate of water removed when Nafion tube is in place}}{\text{rate of water supplied with no Nafion tube}}$$

Equation 5

2.10 Calculating seawater hydrogen concentrations

Hydrogen in the gas stream from the equilibrator was measured using the reducing gas analyzer (RGA) and a chromatogram produced with a peak area proportional to the H_2 concentration in the gas stream. The H_2 concentration is calculated from the peak area using the calibration factor (equation 6). The sample loop volume in the analyser was 1 mL; the gas volume sampled by the loop was corrected to STP (equation 7).

$$H_2\ injected\ into\ analyser\ (nmol) = \frac{Peak\ area\ (PA)}{Calibration\ factor\ (PA/nmol)}$$

Equation 6

$$[H_2] injected\ into\ analyser\ at\ STP\ (nmol/L) = \frac{Hydrogen\ injected\ into\ analyser\ (nmol)}{Volume\ of\ gas\ injected\ into\ analyser\ at\ STP\ (L)}$$

Equation 7

The hydrogen stream represents the composition of the bubbles in the equilibrator.

$$[H_2]_{Air}\ in\ the\ equilibrator\ (nmol/L) = ([H_2] injected\ into\ the\ analyser\ at\ STP(nmol/L)) * \left(\frac{273.15\ (K)}{Equilibrator\ T\ (K)}\right) * \left(\frac{P\ (mbar)}{1013\ (mbar)}\right)$$

Equation 8

The H_2 concentration of the water in the equilibrator is calculated using the Bunsen coefficient, β (Wiesenburg & Guinasso, 1979). The equation for β is a function of temperature and salinity and requires the hydrogen concentration to be expressed as partial pressure (atm); this is the product of the mole fraction of H_2 in the gas mixture and the ambient pressure. The mole fraction of H_2 in the equilibrated air is the same as in the gas flowing to the analyser, so can be calculated from the concentration given in equation 7 multiplied by the molar volume at STP:

$$Mole\ fraction\ of\ H_2\ in\ equilibrated\ air = [H_2] injected\ into\ the\ analyser\ at\ STP\ (nmol/L) * 22.414 * 10^{-9}$$

Equation 9

$$Partial\ pressure\ of\ H_2\ in\ equilibrator\ (atm) = Mole\ fraction\ of\ H_2\ in\ equilibrated\ air * P_{Equil}\ (atm)$$

Equation 10

$$[H_2]_{water}\ in\ the\ equilibrator\ (L\ H_2/L\ water) = Partial\ pressure\ of\ H_2\ in\ equilibrator\ (atm) * \beta(\text{L H}_2\text{ at STP/L water})$$

Equation 11

Correcting this to nmol/L:

$$[H_2]_{water}\ in\ the\ equilibrator\ (nmol/L) = [H_2]_{water}\ in\ the\ equilibrator\ (L\ H_2\ /\ L\ water) \div 22.414 * 10^9$$

Equation 12

To calculate the initial concentration of H_2 in the seawater it is necessary to add together the amount of H_2 (moles) in 1 L of equilibrator water and the amount in the gas phase associated with that 1 L of water.

$$[H_2]in\ seawater\ (nmol/L) = [H_2]_{Air}\ in\ the\ equilibrator * \left([H_2]_{water} in\ the\ equilibrator * \frac{Gas\ flow\ rate}{Water\ flow\ rate}\right)$$

Equation 13

2.11 Flow rates

The flow rate of the water through the equilibrator must be determined so that the relative proportions of the water sample and H_2-free gas can be calculated, which is necessary for the calculation of seawater H_2 calculations (equation 13). A 10% error in the water flow rate would correspond to an error ranging from 8-10% in the calculated H_2 concentration. The gas flow rate was controlled at 2 mL/min (at STP) by a mass flow controller (MKS™).

Two Ismatec™ peristaltic pumps were used in the laboratory experiments to control the water flow rate, one with an analogue display and the other a digital display, herein differentiated by 'analogue' and 'digital'. Only the digital pump was used on the cruise. The peristaltic pump is used to take water from a reservoir of seawater to the equilibrator. The pumps are fitted with Tygon™ tubing because it is impermeable to gases. However, the lifetime of the Tygon™ tubes was considered too short so on the cruise Tygon™ 'Long Flex Life' (LFL) tubes, which were also impermeable to gases, were used because they have a suggested lifetime of 700 hours. The tubes were changed approximately every 7-8 days, to minimize the effects of tube degradation.

2.11.1 Laboratory flow rate calibration

During a 27-hour laboratory experiment (figure 2.6), flow rates were measured by timing how long a 500 mL volumetric flask took to fill with seawater that had been pumped through the equilibrator and dividing by the time interval. The most noticeable change in water flow rate occurred when the pump had been turned off overnight, the subsequent flow rate decreasing from 11.47 to 10.82 mL/min. When the seawater reservoir (5 L) was refilled there was nearly always a significant drop in the flow rate (this is not the case for the final addition, where the flow rate remained unchanged.) Subsequent to these rapid decreases, there was normally a steady increase in flow rate. A calibration factor could not be applied to this increase in flow rates, as the increase was not constant. There appears to be no consistent pattern throughout the 27 hour run, with flow rates sometimes increasing following a refill of water and other times decreasing.

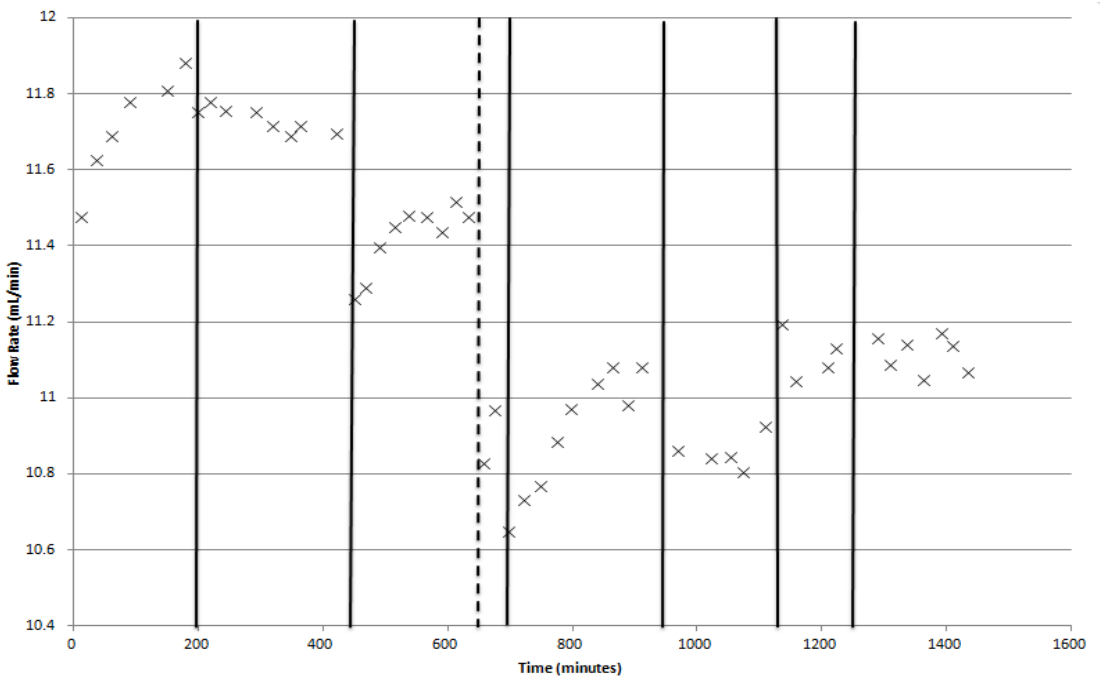

Figure 2.6. Flow rates recorded over a 27-hour period. Solid lines show when the water reservoir was refilled and the dashed line when the pump was stopped overnight.

2.11.2 Temperature effects on water flow rates

On occasions when the water reservoir was refilled there was a drop in the water flow rate. The change in water flow rate could not be caused by the change in water level, because a rise in the water level in the supply reservoir would decrease the pressure head between the equilibrator and the reservoir and likely lead to a flow rate increase.

It appears that a change of water temperature causes the changes in flow rate. In figure 2.6, the addition of colder water (that has not had time to equilibrate to the room temperature) leads to an almost immediate drop in the flow rate. This decrease in flow rate may be due to the decrease in temperature of the water, leading to a change in the elastic properties of the tubing and the tube not being completely closing with some leakage of backwards.

In the field, changes in seawater temperature of this magnitude (~5 - 10°C) did not occur on such short timescales so the extreme changes in the flow rate that were observed in the laboratory are unlikely to have occured.

2.11.3 Water flow rates in the field

At sea, flow rates were calculated by timing, with a digital stopwatch, how long a 500 mL volumetric flask took to fill with sample water that had been through the equilibrator. Water was sampled from a reservoir with a constant level to avoid the potential problem of a decreasing flow rate when the reservoir level was increased. Measurements at sea were made daily and are shown in Figure 2.7a, along with the times when new tubes were installed and when flow rate adjustments were made. A "flow rate adjustment" of the peristaltic pump aimed to get the pumped flow rate to the optimal 14 mL min^{-1}. By entering the last known flow rate into the pump's control system, an automatic adjustment of the motor's RPM gave a rate closer to 14 mL min^{-1}. The adjusted flow rate was closer to the desired set flow rate but rarely identical, so it was

volumetrically re-measured. The magnitude of the adjustment was based on the last known flow rate, that on some occasions was made 24 hours earlier. Flow rates varied between 10.25 and 14.93 mL min^{-1}.

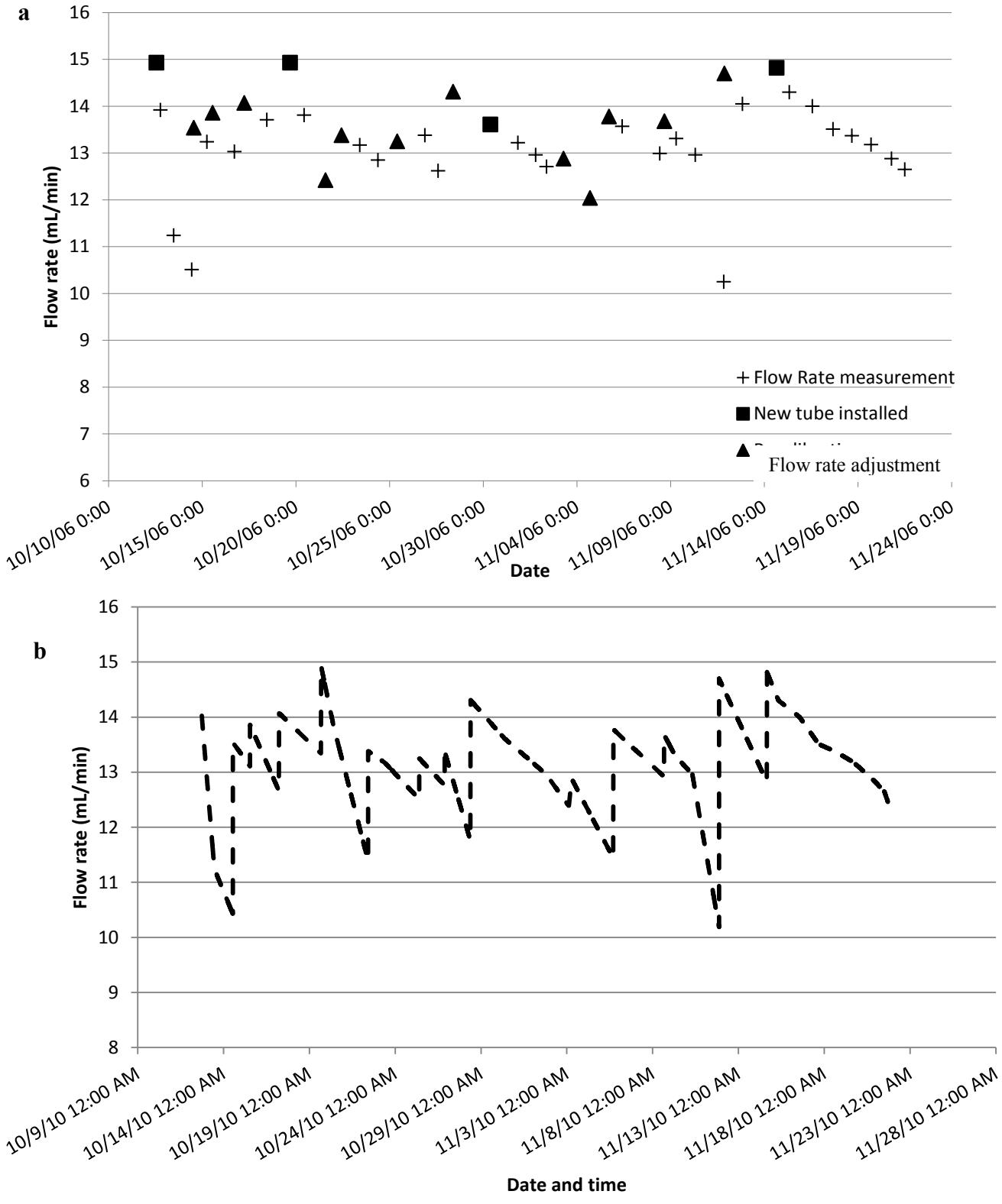

Figure 2.7a and b. **a.** Flow rates measured during the AMT20 cruise. **b**. Interpolated flow rates calculated for each H_2 measurement.

When a new tube was installed it was run for a few hours without any H_2 measurements being made, it was then adjusted to give a flow rate close to 14 mL min^{-1}, which was volumetrically measured. It was this last measurement that was recorded.

Some flow measurements were made less frequently than every 24 hours, and flow rates changed as much as 2.7 mL min^{-1} from day to day, so it was decided that an interpolated flow rate would be calculated for each hydrogen measurement. The circumstances underwhich the preceding and subsequent flow rates were measured determined how the interpolated values were calculated. It is assumed that the deterioration of the tubes will lead to a decrease in the flow rate. For periods during which there was more than one sequential "un-calibrated" point, a linear regression was used. For times when only one "un-calibrated" data point followed a flow rate adjustment or new tube, a linear rate of deterioration between the two measurements was used. In both instances the slope is extrapolated until there is either a flow rate adjustment or a new tube is installed.

When a flow rate adjustment was made many hours after a measurement, it was necessary to interpolate between the two flow rates because flow rates were unknown during this period. It was assumed that the flow rate adjustment would increase the flow rate from the last measurement to the optimal 14 mL min^{-1}. The unmeasured flow rate, immediately prior to adjustment, is obtained by subtracting the adjustment increase/decrease from the measured flow rate after adjustment. For example, if the last known flow rate measurement was 12.5 mL min^{-1} then the flow rate adjustment would have increased the flow rate by 1.5 mL min^{-1} (to give a flow rate of 14 mL min^{-1}). If the measured flow rate after flow rate adjustment was 13.7 mL min^{-1}, then the flow rate just before flow rate adjustment is determined to be (13.7 - 1.5 mL min^{-1}) 12.2 mL min^{-1}.

Although the pump's flow rate was usually adjusted regularly, there are periods when this was not the case. Figure 2.8 shows seven consecutive flow rate measurements made without a flow

rate adjustment, the high R^2 value (0.985) given to the linear regression of flow rate versus time gives credence to the assumption that there is a linear change in flow rates from one measurement to the other.

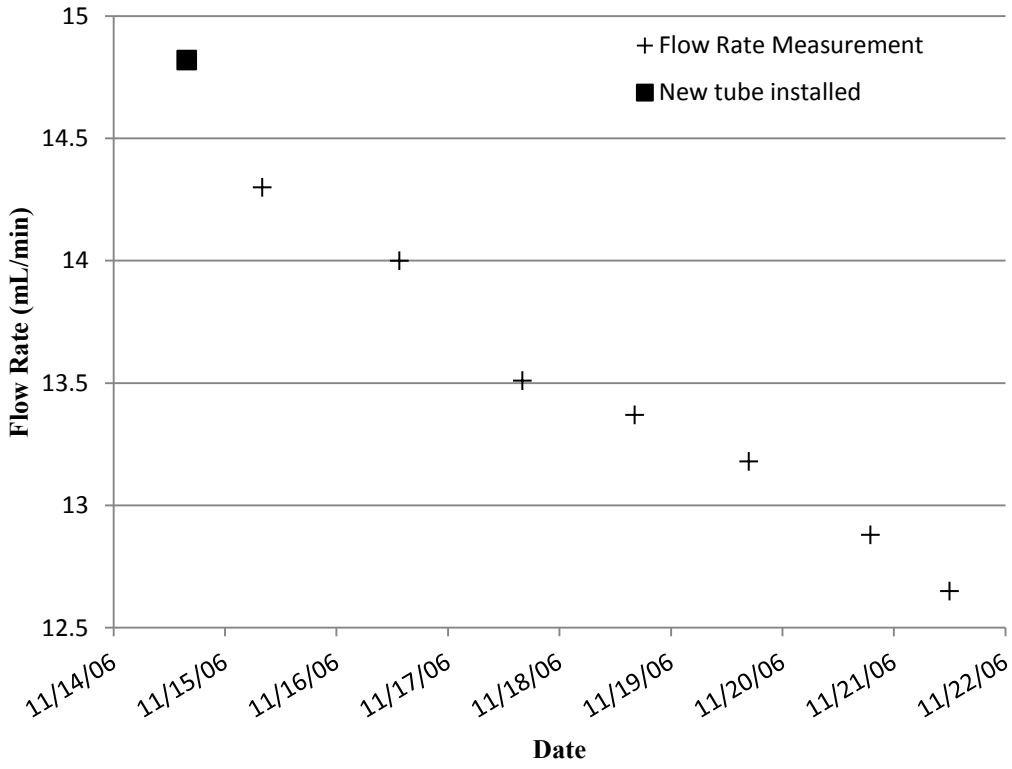

Figure 2.8. Flow rate measurements made subsequent to a new tube installation.

2.12 Temperature

The temperature of the sample loop in the reducing gas analyser was measured using a custom made thermometer, that consisted of a thermistor with a digital readout. The temperature of the equilibrator was measured using a thermocouple placed in the water bath that surrounded the equilibrator and was recorded directly onto the memory module of the valve controller. Temperature measurements in the equilibrator allowed the air flow rate (mL/min) in the equilibrator to be calculated from the flow given by the mass flow controller (equal to 2 mL/min at STP). The air-to-water ratio in the equilibrator can then be calculated. Calculation of the

Bunsen coefficient also uses the equilibrator temperature. The sea surface temperature (SST) was also recorded for calculation of the solubility of H_2 in the seawater. The sea surface temperature was measured with a hull mounted SBE38 thermometer (SeaBird Electronics Inc), and recorded every minute.

The sample loop thermometer located inside the analyzer was calibrated by submerging the sensor into stirred iced water until the readout settled. It was found that the thermometer needed to be corrected by -0.6°C. The thermocouple was calibrated using the custom made thermometer, as this was deemed to be most accurate (±0.1°C). This calibration was performed regularly throughout the day by simultaneously measuring the equilibrator temperature and applying the correction to the recorded data retrospectively. It should be noted that the difference between the two values was assumed to be the same until the next calibration.

2.13 Efficiency calculations

The efficiency of the equilibrator at extracting H_2 from a water sample was determined with liquid standards. A liquid standard was produced by bubbling a 5 ppm H_2 gas standard at a high flow rate (110 mL/min) through a seawater sample for a minimum of 10 minutes. Laboratory experiments determined that the liquid standard became fully equilibrated after < 5 minutes. The extraction efficiency is defined as the percentage of the calculated concentration of the liquid standard that is measured by the analyzer. The extraction efficiency for each day was applied to the hydrogen measurements made from the time halfway between the previous efficiency measurement and the current efficiency measurement to halfway to the next efficiency measurement.

2.14 Blanks

Liquid blanks were produced by bubbling air, which was scrubbed of H_2 and CO, at a high flow rate (110 mL/min) through a seawater sample of ~500 mL for a minimum of 10 minutes. The blanks enabled the calculation of the H_2 introduced to the sample from the equilibrator and other equipment. The apparent H_2 concentration of the blank after it had passed through the system ranged from 0.06 to 0.12 nmol/L. The blanks were measured daily, and the peak area measured for each blank was used as a correction for hydrogen measurements made from the time halfway between the previous blank measurement to halfway to the next blank measurement.

2.15 Fluorescence measurements

Fluorescence was measured using a chlorophyll fluorometer (WETLabs Wet Star) that was plumbed into the ship's non-toxic seawater supply (located at ~7 m depth). Water samples were collected from the non-toxic supply for chlorophyll analysis to calibrate the fluorometer. In this study, only the raw fluorescence is used.

CHAPTER 3 **DATA PROCESSING**

During the cruise, some measurements were made on samples contaminated by the ship or were considered spurious in another way. This chapter will outline the criteria for selecting which measurements from underway samples are free from contamination and represent measurements of authentic samples.

3.1 Gaps in the data

Throughout the cruise there were occasions when measurements could not be made. For example, it was not permitted to make H_2 measurements when the ship was within the 200 nautical-mile exclusive economic zones of the Azores and Ascension Island, accounting for breaks in the data from ~35°N to 40°N and from ~7°S to 10°S respectively.

Furthermore, there were two occasions (between 18.7°N and 19.7°N, and 23.4°N and 23.4°N) when a hydrophobic filter became blocked and both H_2 and CO peak areas dropped to almost zero. The hydrophobic filter was fitted to the top of the bubble separator to prevent water droplets, formed by bubbles bursting in the bubble separator, from entering the reducing gas analyzer. When the filter was replaced the H_2 and CO peak areas returned to normal levels.

There were also instances when the data for one or more parameters were not recorded on to the memory drive; such cases were labeled “error”. It was not possible to complete all necessary calculations if any essential data were missing, so the entire measurement was discarded. Also, when both the H_2 and CO peak areas were zero, it was deemed that there was an error in the analyser or in recording the data.

3.2 Contamination from the ship

To protect a ship's submerged hull from corrosion, sacrificial zinc anodes, which are preferentially corroded, are commonly fitted to the structure below the water line. However, the corrosion of these anodes creates a plume of hydrogen-rich water, which can contaminate water samples. The two zinc anodes that were immediately forward of the *RRS James Cook's* seawater intake were removed prior to the cruise, giving us confidence that the water sampled while the ship was underway would be free of this contamination. However, the anodes downstream of the intake and on the opposite side of the ship had to remain and we have evidence that these anodes contaminated samples when the ship was on station and when maneuvering onto station. To illustrate that the ship contaminated waters while it was on station, surface hydrogen data are shown (figure 3.1) for a set of eight consecutive stations where measurements were made during both two hours before the station, and at least one hour on the station.

Further evidence of contamination from the ship can be observed in H_2 concentrations of discrete samples taken with Niskin bottles from the surface to 10 m (figure 3.2). Hydrogen concentrations were highly variable, but some concentrations were an order of magnitude higher than nearby underway concentrations. To avoid damaging the CTD rosette it was necessary for the ship, while on station, to have the wind on the starboard side, where the CTD rosette is launched into the water, allowing the ship to drift away from the instrument. However, this led to the Niskin rosette taking surface water that may have been contaminated by the ship.

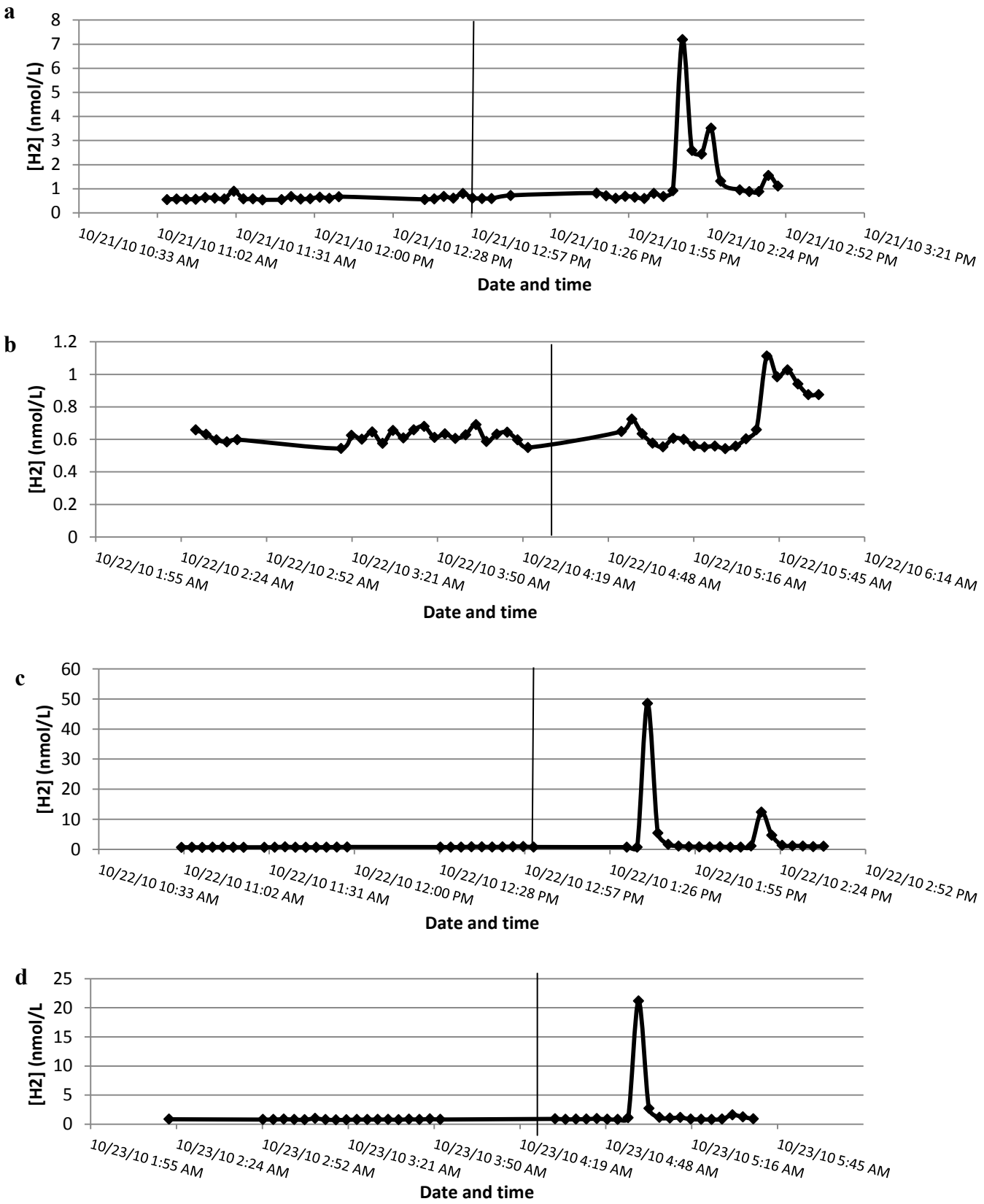

Figure 3.1. H_2 measurements made on samples taken from the ship's underway system while approaching a station. The vertical line identifies when the ship was officially on station.

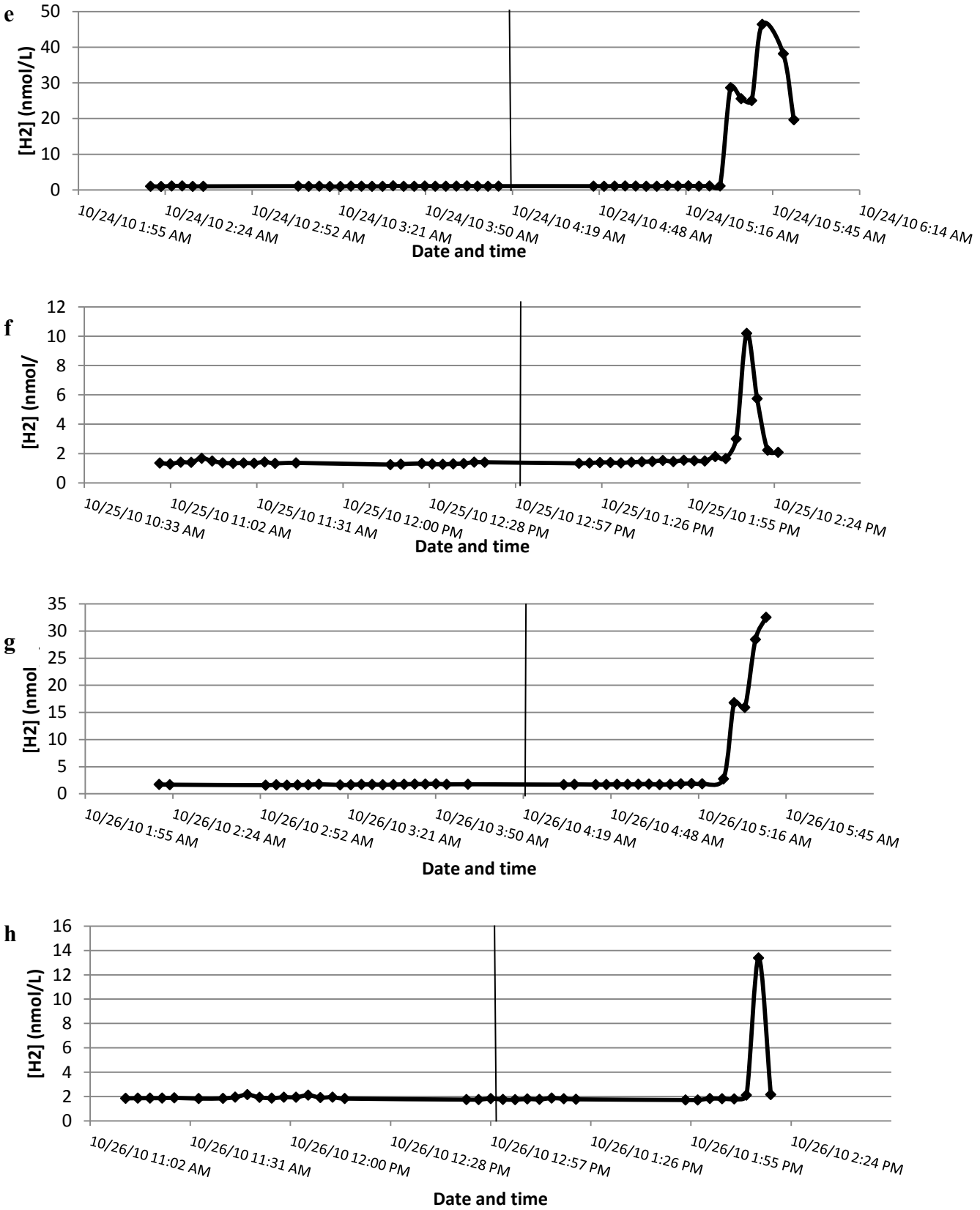

Figure 3.1. H_2 measurements made on samples taken from the ship's underway system while approaching a station. The vertical line identifies when the ship was officially on station.

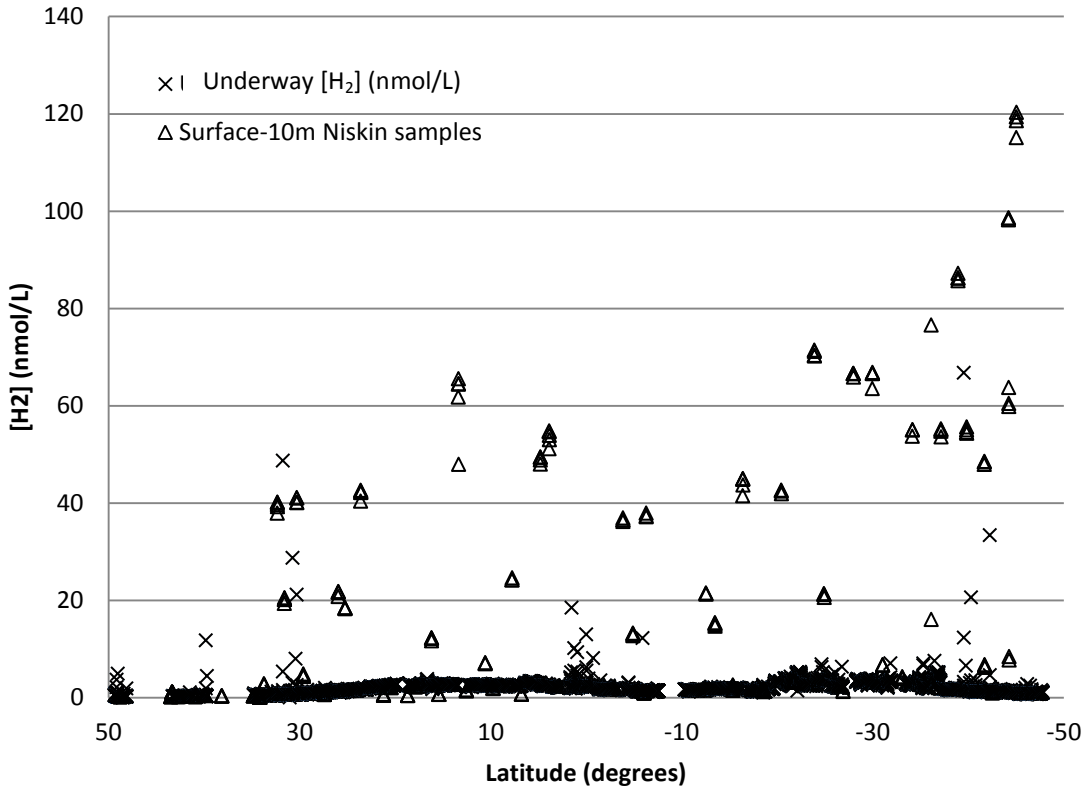

Figure 3.2. Hydrogen measurements from Niskin samples taken from the surface to 10m and underway hydrogen measurements.

Any measurements made from the ship's seawater intake while at station (as noted in the captain's log), are not included as underway measurements. Using this criterion, any contamination from the ship while at station or maneuvering at station is not presented. Furthermore, there is little resolution lost from the underway transect as the ship was stationary.

Analysis of samples taken from the Niskin rosette was started immediately, taking on average 2 hours to complete. Because the ship would leave the station immediately after the rosette of Niskin bottles was onboard, it would be clear of contaminated station water by the time the analysis of discrete samples was complete, so underway measurements could be resumed immediately.

There were instances when the ship travelled through its own wake (figure 3.3a) or turned quickly, which resulted in a spike in the H_2 concentration from the underway-sampling system (figure 3.3b). It should be noted that the time between water being sampled at the ship's intake and the measurement made by the analyser is approximately 15 minutes. Each marker in figure 3.3a represents a GPS location taken every minute, and the beginning of the loop is 1700 hours. The dotted line in figure 3.3b represents the time when the water sampled at 1700 hours was analysed (after the 15 minute delay). In total 17 measurements were identified as contaminated from the ship passing through its wake and will not be included in our analysis. It should be noted that our findings are in direct contradiction with those of Sester *et al.* (1982), who observed no contamination from the ship when water from the ship's wake were analysed.

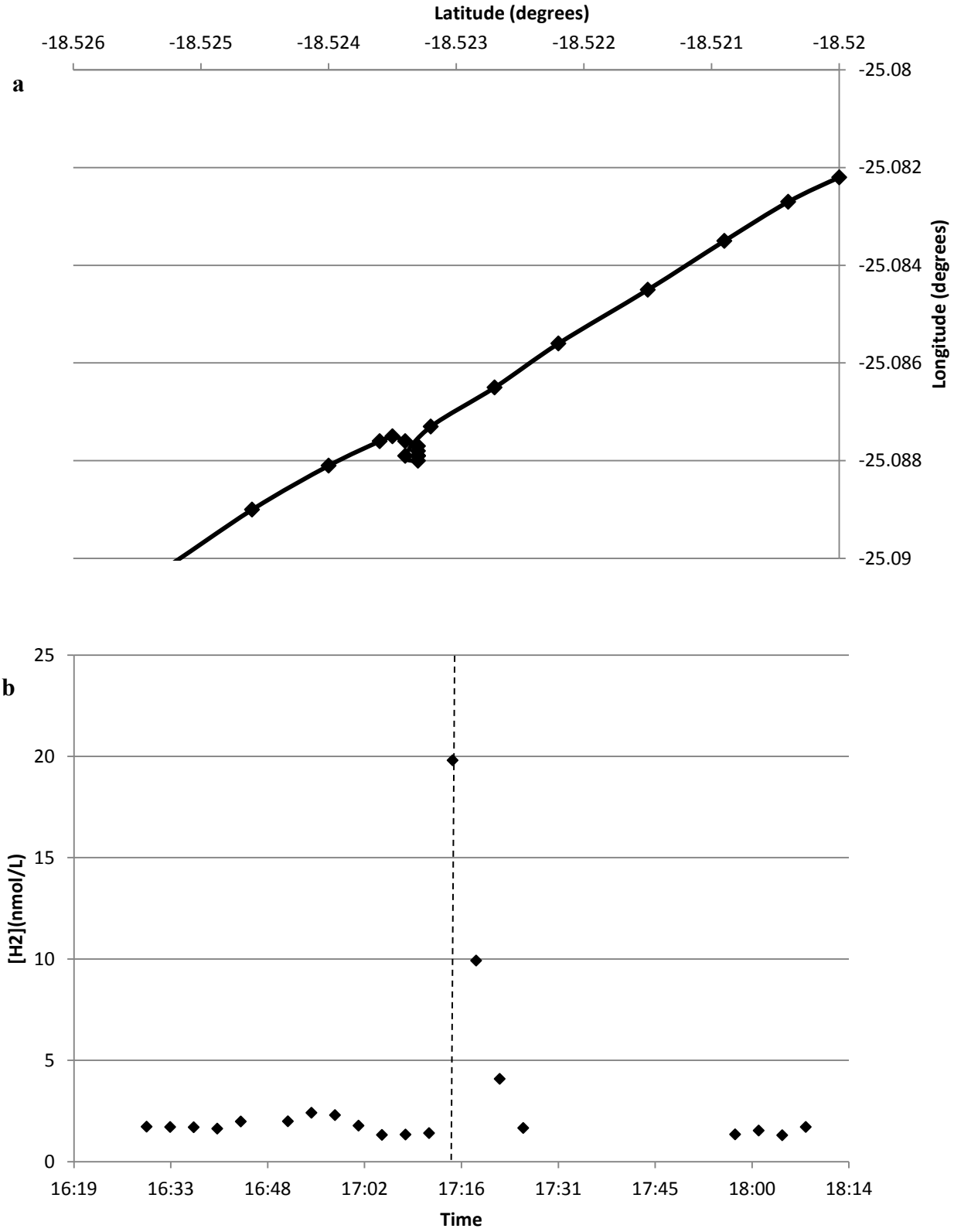

Figure 3.3 **a**. Cruise track of *RRS James Cook* on 12 November 2010, way points are one minute apart. **b**. Hydrogen concentrations measured during the same period, the dashed line represents when the water sampled at the time the ship crossed its wake would be measured.

3.3 Anomalous hydrogen peaks

There were occasionally extremely high spikes that could not be accounted for; these will be referred to as "anomalous" (figure 3.4a). These anomalies were identified by applying a running median (in blocks of 11 measurements) to each underway measurement (Tukey, 1977; R Development Core Team, 2012). All measurements that were 3.6 standard scores above or below the median were identified as anomalous and are not used in our analysis (see figure 3.4b). A standard score is defined in equation 6, where x is the individual measurement, μ is the median of the 11 measurements and σ is the standard deviation of the 11 measurements. It should be noted that changing the size of the block, between 3 and 101 had no effect on the results. Using this criterion, 23 measurements were identified as anomalous.

$$z = \frac{x - \mu}{\sigma}$$

Equation 6.

In addition to using a running median function, the smooth function in "R" was employed on all data including those measurements that had been identified as anomalous. The smooth function is similar to the running median, but uses blocks of 3 values and repeats the running median until the numbers converge. Again, measurements that were 3.6 standard scores above the median were identified as anomalous. This method identified the same 23 measurements, and the remaining measurements are shown in figure 3.4c. The parameters of both of these methods are very conservative, with the chance of a measurement being 3.6 standard scores above the median as 6285 to 1. Thus, only the very extreme outliers are identified with these methods and it is likely that measurements made prior or just after the spike, which may be higher than authentic concentrations, remain in the dataset.

Because the instrument does not respond instantaneously to a change in H_2 concentration, there would always be a second, lower peak following an initial spike. On account of the very conservative criterion used to identify the largest spikes (of which there were 23 identified), this approach, in most cases, did not pick up these secondary points. An additional 19 points have been omitted for this reason. Thus, the anomalous samples amounted to 42 in a total of 6040 remaining underway measurements of dissolved H_2 in surface waters.

In an effort to identify the cause of the spikes in H_2, the ship's track as well as the speed of the ship was analyzed. There was no consistent correlation in the H_2 spikes and the ship's movements. To assess whether an air bubble drawn into the equilibrator was the cause of these spikes, the size of the bubble that would lead to a doubling of H_2 concentration was estimated. The distribution coefficient of H_2, the ratio of the H_2 concentration in equilibrated air to that in water, was calculated at about 60. The analyzer loop has a volume of 1 mL, which represents the equilibration of 7 mL of water. Therefore, in order to double the peak area of H_2, the bubble would have to contain the equivalent of another 7 mL of water. Using the distribution coefficient, the volume of the air bubble would be 7/60 mL, which equals approximately 120 μL. This would mean that the diameter of the air bubble that would lead to a doubling in the peak area is in the order of 6 mm. It seems unlikely that a bubble this large could get drawn into the equilibrator. Furthermore, it would be expected that larger numbers of smaller bubbles would also be observed.

Of all 6057 underway measurements, 17 have been identified as contaminated by the ship while underway, through rigorous testing 42 have been determined to be outliers and the remaining 5998 are recognized as authentic underway H_2 concentrations along the AMT20 transect and are shown in figure 3.5.

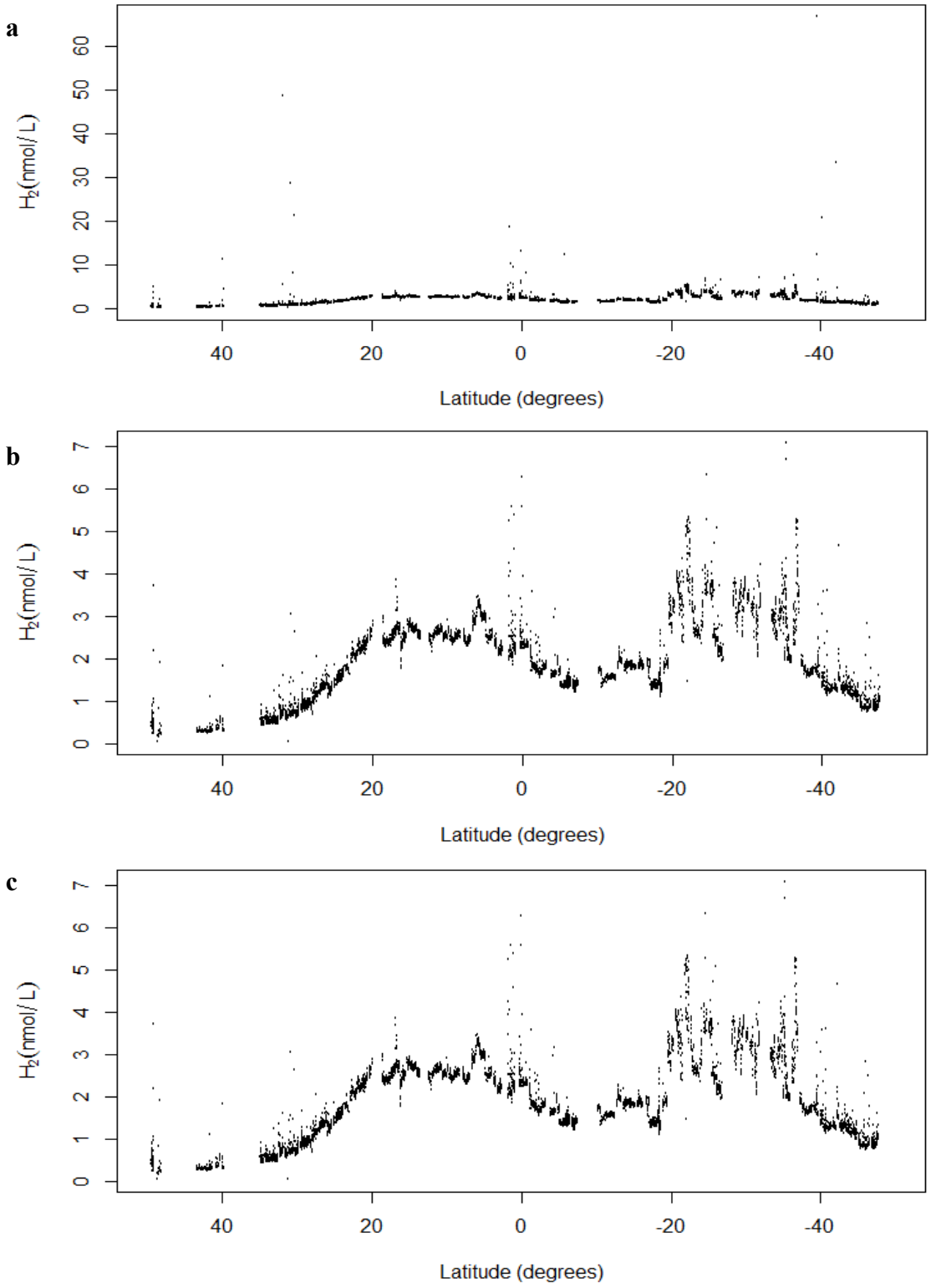

Figure 3.4. **a**. Hydrogen concentrations with all underway measurements. **b**. Hydrogen measurements with anomalous measurements removed using the "running median" function. **c**. Hydrogen measurements with anomalous measurements removed using the "smoothing" function.

CHAPTER 4 **PRELIMINARY DISCUSSION OF RESULTS**

Nitrogen fixation rates (determined by $^{15}N_2$ incubations), wind speed, chlorophyll fluorescence, temperature and salinity were measured in addition to H_2 concentrations along the Atlantic Meridional Transect (AMT). Although it is beyond the scope of this Master's thesis to discuss in depth the relationship of H_2 concentrations with this range of parameters, here is presented a preliminary overview of some of these relationships. It should be noted that nutrient concentrations from water samples taken on the cruise are not currently available, so data are presented from the World Ocean Atlas (WOA) (Boyer et al., 2006).

4.1 Hydrogen concentrations along the AMT20 transect

Hydrogen concentrations had a bimodal distribution along the AMT20 transect (figure 4.1a). Concentrations measured while the ship was underway ranged from 0.1 to 5.4 nmol/L, although the majority (96%) of these are in the range 0.3 to 3.5 nmol/L. Much more variability is observed in H_2 concentrations between 20 and 37°S, which may be a result of increased springtime plankton growth in this region.

Hydrogen saturation levels between 10°N and 20°N, a region along the North Atlantic section of the cruise track with the highest H_2 concentrations, were on average 780% (figure 4.1b). In a region in the South Atlantic with elevated H_2 concentrations, between 20°S and 30°S, H_2 saturation levels were on average 940% although it should be noted that these levels were much more variable. Saturation levels observed in this study are generally higher than those reported in the literature. Seiler and Schmidt (1974), for example, reported average saturation levels of

~400% in the North and South Atlantic Oceans. On a transect in the tropical North Atlantic, Herr and Barger (1978) found that the mixed layer had average saturation levels of 190%. Furthermore, they state that only 3% out of 278 H_2 measurements (from all depths) had saturation levels of 400% or higher along a 4800 nautical-mile transect. A study of the Mediterranean Sea found typical surface H_2 saturation levels of 300 – 500% (Scranton, Jones, & Herr, 1982). While these Mediterranean Sea saturation levels are lower than our results, plankton net tows found no *Oscillatoria* (now *Trichodesmium*) in the Mediterranean Sea, implying that H_2 production from these diazotrophs was not occurring. From continuous surface measurements of H_2 in the ocean waters off Baja California, Setser *et al.* (1982) found that the majority of H_2 concentrations were at, or just above atmospheric equilibrium. However, in one warmer water mass, saturation levels in the range of 240 – 350% were observed.

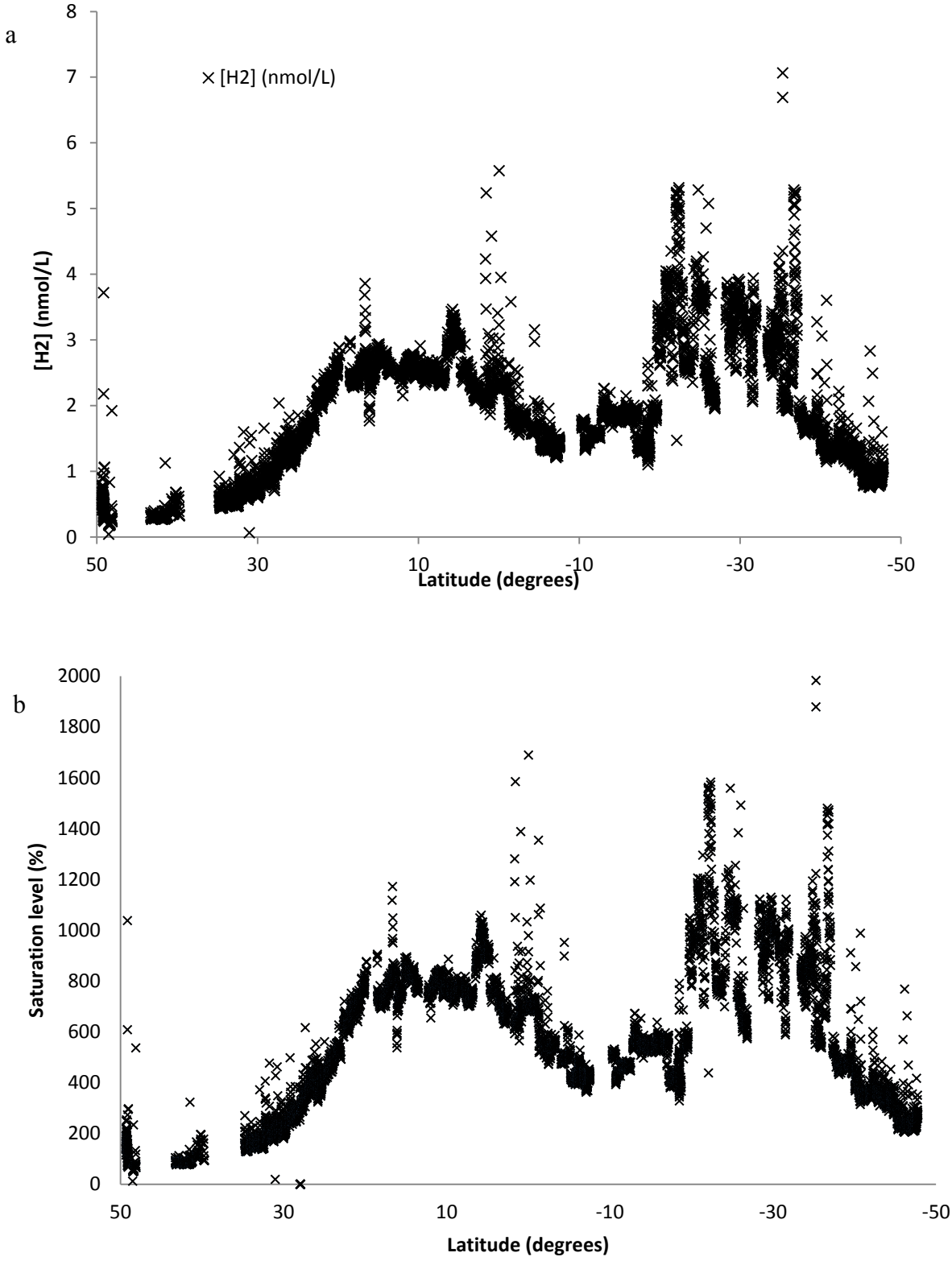

Figure 4.1.a. Underway hydrogen concentrations (nmol/L) along the AMT20 transect with all 42 anomalous measurements removed. b. Underway hydrogen saturation levels (%).

4.2 Hydrogen as an indicator of nitrogen fixation rates

A major aim of this study was to establish whether H_2 concentrations could serve as an indicator of nitrogen fixation. It has been demonstrated on previous AMT cruises (specifically AMT17) that nitrogen fixation rates (determined from $^{15}N_2$ incubations) are considerably higher in the North Atlantic than the South Atlantic, see figure 4.2a (Moore *et al*., 2009a). The authors state that nitrogen fixation in the North Atlantic is dominated by the larger size fraction of diazotrophs, in particular *Trichodesmium* filaments (figure 4.2b and 4.2c). They suggest that low iron concentrations in the South Atlantic limit growth of *Trichodesmium* and thus nitrogen fixation. Furthermore, a compilation of *Trichodesmium* filament counts from 8 different AMT cruises showed high abundances between 0 and 15°N (Tyrrell *et al.,* 2003), but almost complete absence between 0 and 30°S. Based on nitrogen fixation data from AMT17 (figure 4.2), the H_2 peak in the South Atlantic was not expected and does not correlate with these previously measured nitrogen fixation rates. This may be a result of the two cruises sampling in different regions of the South Atlantic, with AMT17 on a more easterly cruise track in a region with perhaps with less nitrogen fixation.

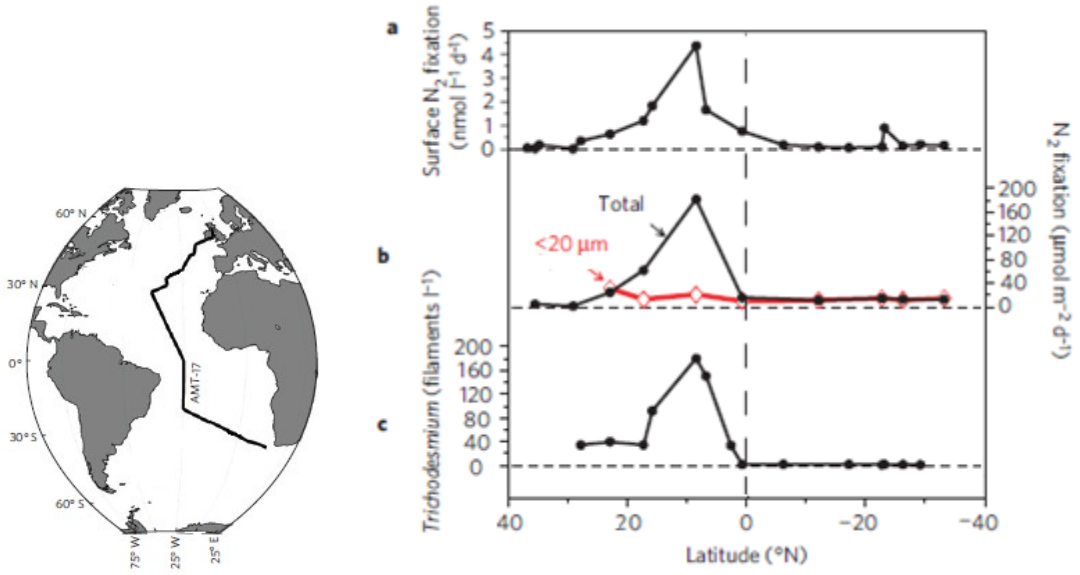

Figure 4.2. Transect data from AMT17. A, Surface N_2 fixation rate. B, Total and <20µm integrated water column rates of N_2 fixation. C, Surface *Trichodesmium* distribution. Adapted from "Large-scale distribution of Atlantic nitrogen fixation controlled by iron availability," Moore *et al.* (2009a)

A study in the North and South Atlantic by Grosskopf *et al*. (in press) found that the established method of measuring N_2 fixation rates, by injecting a bubble of $^{15}N_2$ into a discrete water sample, underestimated rates compared to a "dissolution method" (see section 1.3.2). Furthermore, they suggest that this underestimation varies depending on the dominant diazotrophs within the community. In regions where *Trichodesmium* is dominant, for example, the underestimation of nitrogen fixation was on average 62%, but in regions where unicellular and symbiotic cyanobacteria are dominant the dissolution method yielded N_2 fixation rates that were six times higher than bubble method. Using the "dissolution method", regions that were previously believed to have low rates of nitrogen fixation, including the South Atlantic Gyre (at 38°S) and the Falkland Current (at 44°S), showed sizeable nitrogen fixation rates (0.44 ±0.1 and 0.54 ±0.1 µmol N m^{-3} d^{-1} respectively). Nitrogen fixation rates measured using the bubble injection method were considerably lower, 0.10 ± 0.01 and 0.18 ± 0.03 µmol N m^{-3} d^{-1} for the South Atlantic Gyre and the Falkland Current respectively. Therefore, it is feasible that the nitrogen fixation rates measured by Rees (Plymouth Marine Laboratory), using the bubble injection method, in this

study underestimated rates in regions where unicellular and symbiotic diazotrophs are the dominant within the community.

There was very little correlation between H_2 concentrations and surface $^{15}N_2$ fixation rates measured during AMT20 (figure 4.3a and b). Furthermore, the higher rates of N_2 fixation have very large errors associated with them. Direct comparison of surface N_2 fixation rates and H_2 concentrations from the same Niskin bottle was unfeasible due to contamination of surface H_2 measurements. Therefore, the five H_2 concentrations measured immediately prior to arriving on station are used in calculating a linear regression. Figure 4.3b shows H_2 concentration plotted against N_2 fixation rates, with weighted ($r^2 = -0.009$) and unweighted ($r^2 = 0.299$) linear regressions. The weights used for this regression are calculated using $\frac{1}{w^2}$, where w is the error associated with each N_2 fixation measurement. In this study the distribution of nitrogen fixation rates is less well defined than in Moore *et al.* (2009a), with a more sporadic distribution.

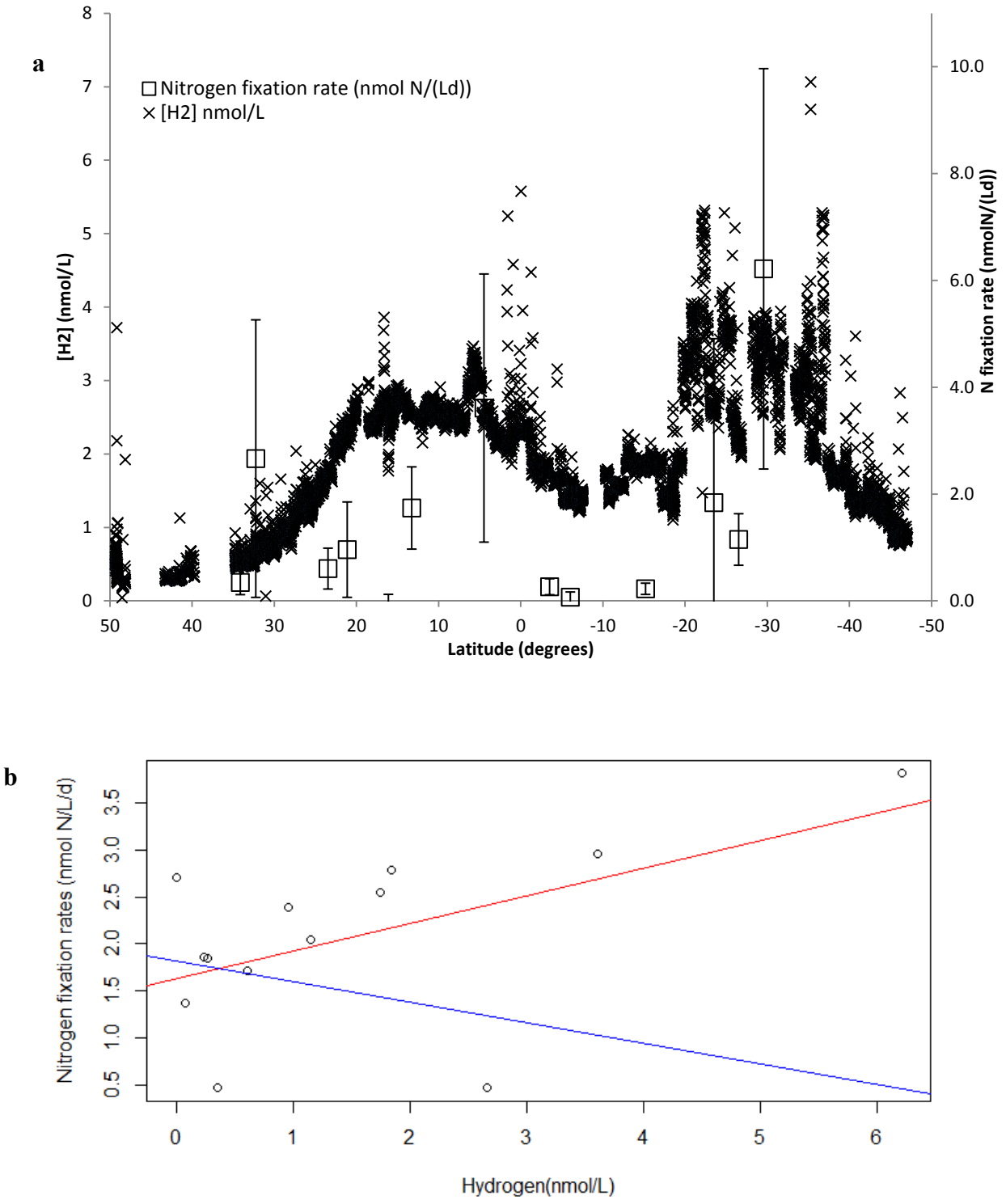

Figure 4.3.**a** Hydrogen concentrations and N_2 fixation rates calculated from $^{15}N_2$ incubations with errors (±2 standard deviations) courtesy of Dr Andy Rees, Plymouth Marine Laboratory. **b**. H_2 concentrations and N_2 fixation rates with unweighted (red) and weighted (blue) linear regressions.

4.3 Distribution of nitrate and phosphate

Nitrate data are shown from the World Ocean Atlas along the AMT20 transect (figure 4.4b). Surface nitrate concentrations were lowest in the subtropical gyres and increased polewards. At ~35°S, where surface nitrate concentrations begin to increase, there is a drop in H_2 concentrations and the variability of H_2 concentrations. In laboratory studies, the presence of nitrate has inhibited nitrogen fixation (Holl & Montoya, 2005). Therefore, the presence of nitrate may result in this region may mean that diazotrophs are no longer competitive and thus a decline in nitrogen fixation would be observed (and also a decrease in hydrogen production). This correlation may also be due to higher concentrations of nitrate inducing increased growth of H_2-consuming organisms.

Phosphate concentrations are distributed similarly to nitrate along this transect, with the lowest concentrations in the subtropical gyres (figure 4.4c). Phosphate is known to limit nitrogen fixation in some regions (Karl *et al.*, 1997), but in our study the highest H_2 concentrations (and thus inferred nitrogen fixation rates) occur in regions with the lowest inorganic phosphate concentrations. For diazotrophs in these regions, it may be that efficient recycling of organic phosphate is sufficient to sustain nitrogen fixation (Wu *et al.*, 2000).

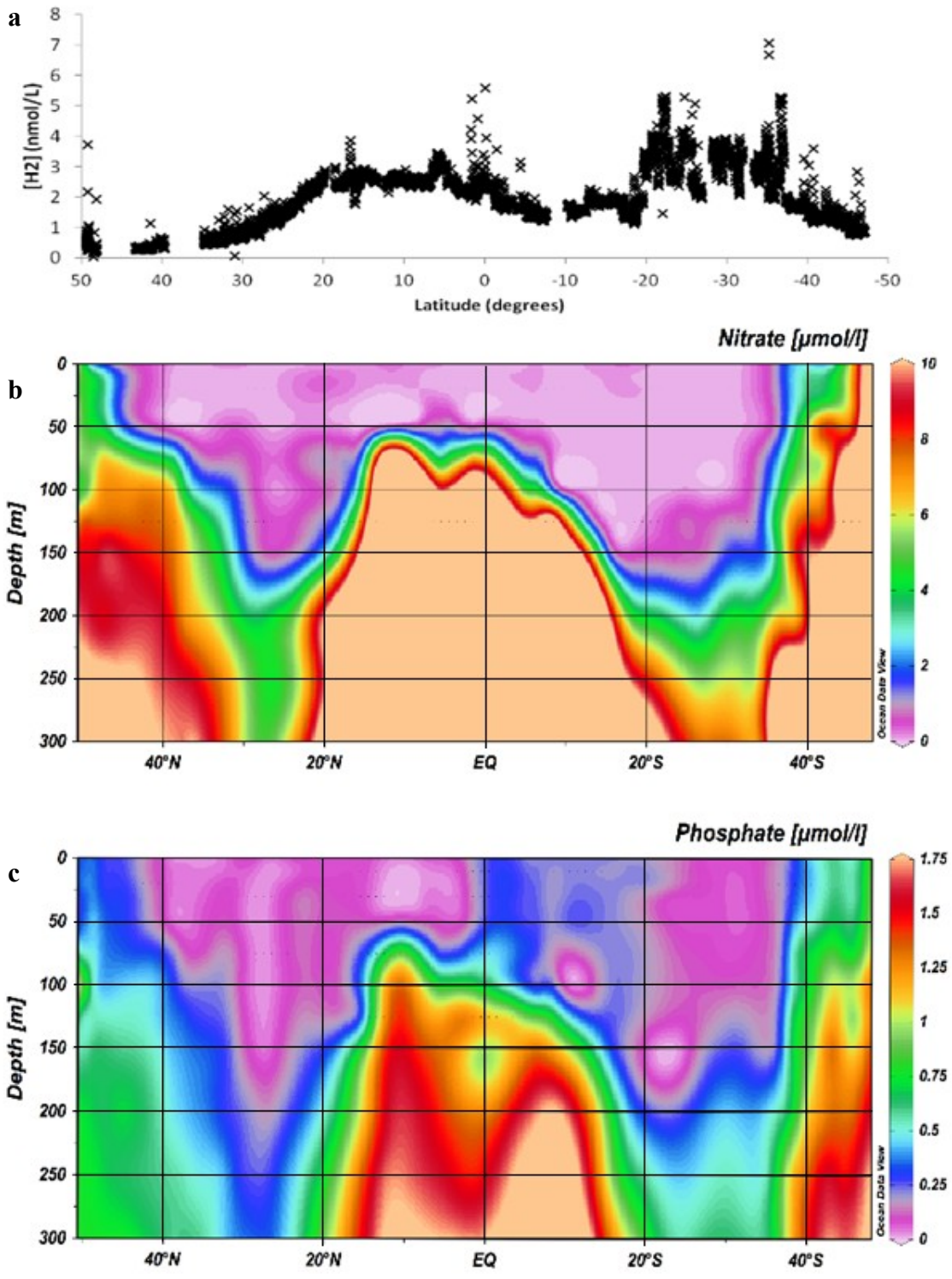

Figure 4.4. **a**. Hydrogen concentrations, **b**. nitrate concentrations and **c**. phosphate concentrations along the AMT20 transect; nitrate and phosphate data are from the World Ocean Atlas (up to 2009).

4.4 Fluorescence and hydrogen concentrations

Chlorophyll fluorescence is commonly used as a proxy for phytoplankton biomass (Lavigne *et al.*, 2012). However, the relationship between fluorescence and biomass is a complex one, and dependent on light exposure history, nutrient status and taxonomic composition (Cullen, 1982). For these reasons, fluorescence measurements in this thesis will be regarded as only a semi-quantitive measure of biomass. Fluorescence was measured semi-continuously with a chlorophyll fluorometer connected to the ship's underway water supply (figure 4.5). It should be noted that the fluorescence data are raw fluorescence readings, without calibration or blanks, therefore, only relative chlorophyll fluorescence will be discussed. As with the WOA nitrate and phosphate data, relative chlorophyll fluorescence increases rapidly at ~35°S where H_2 concentrations become much less variable. The high fluorescnce measurements, relative to other regions of the transect, suggest increased biomass. This may be further evidence for the hypothesis that the decrease in variability of hydrogen concentrations is due to either the growth of non-diazotrophs or H_2-consuming bacteria.

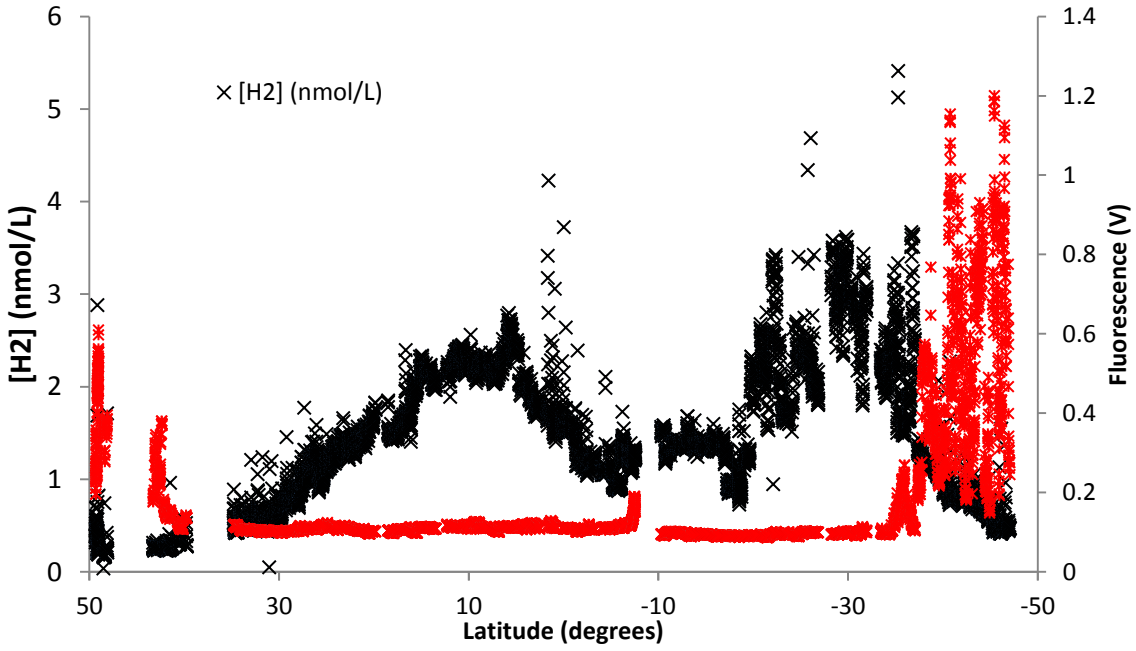

Figure 4.5. Fluorescence (V) and hydrogen concentrations measured on AMT20.

4.5 Wind speed and hydrogen concentrations

Wind speed was measured with an anemometer fixed above all other instrumentation on the ship's meteorological platform. There is considerable correlation between H_2 concentrations and wind speed from 6°N and 22°S (see figure 4.6a). For this region, the highest H_2 concentrations were measured during periods of low wind velocity. It is possible that this is due to a slower gas transfer velocity leading to less ventilation of H_2 and thus higher concentrations. In addition or alternatively, blooms of *Trichodesmium,* which are known to develop under calm conditions, may lead to increased H_2 production (Hood, Coles, & Capone, 2004). An inverse relationship is observed for wind speeds less than ~15 m/s (figure 4.6c), after which the H_2 concentrations remain at a minimum while wind speeds continue to increase. The inverse relationship between 0 and 15 m/s has an r^2 of 0.44 ($n = 832$, $P < 0.01$), meaning that 44% of the variability in these data is accounted for by this linear regression (see figure 4.6c). Because the various other factors that determine the H_2 concentration are not taken in to account, factors including mixed layer depth, H_2 production and consumption rates and composition of the diazotroph community, a high r^2 value is not expected. A very similar relationship is observed with wind speeds between 0 and 15 m/s and hydrogen saturation level ($r^2 = 0.44$, $n = 832$, $P < 0.01$) in the same region (figure 4.6d). This is not surprising as saturation levels and H_2 concentrations are very similar in this study. There appears to be no link in other regions along the AMT20 transect between wind speed and H_2 concentration.

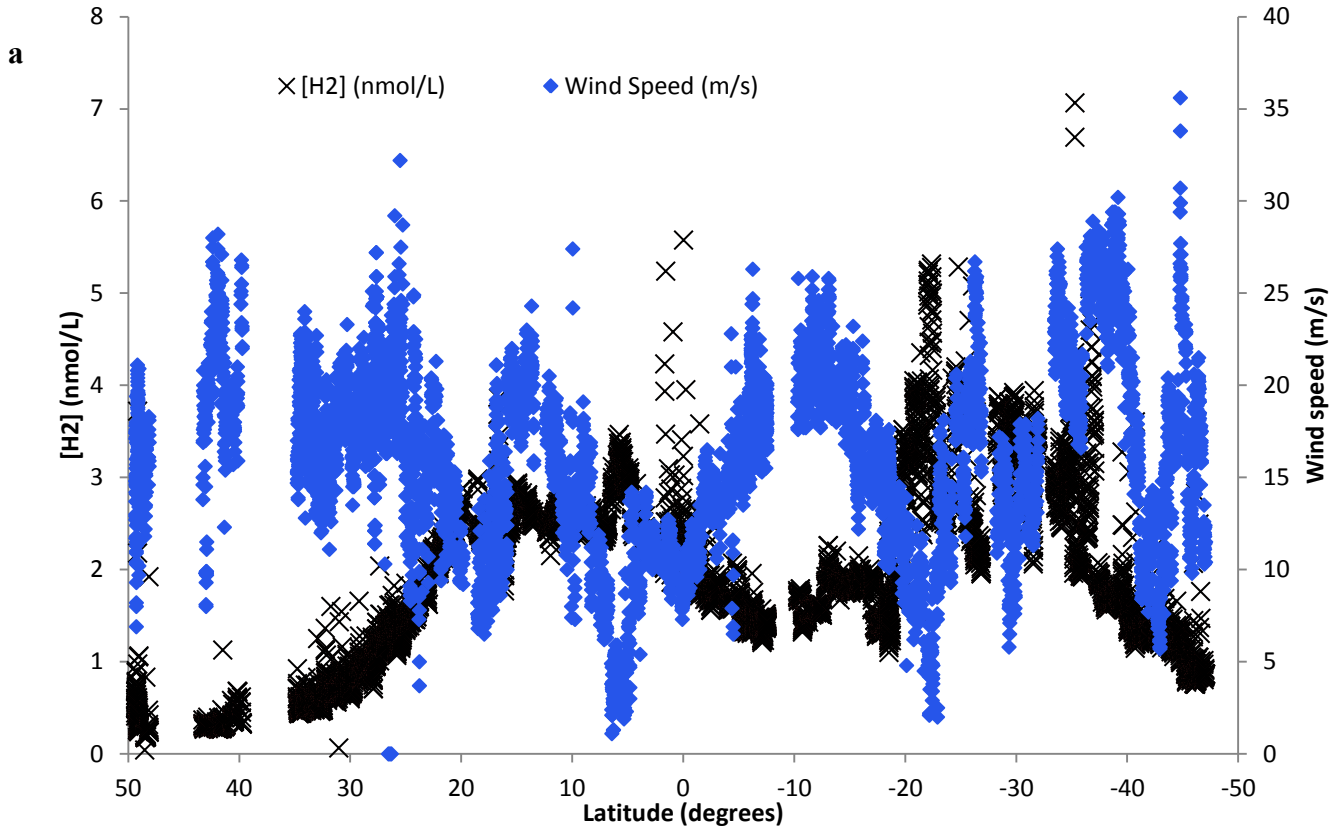

Figure 4.6a. Wind speed (m/s) and hydrogen concentrations measured on AMT20.

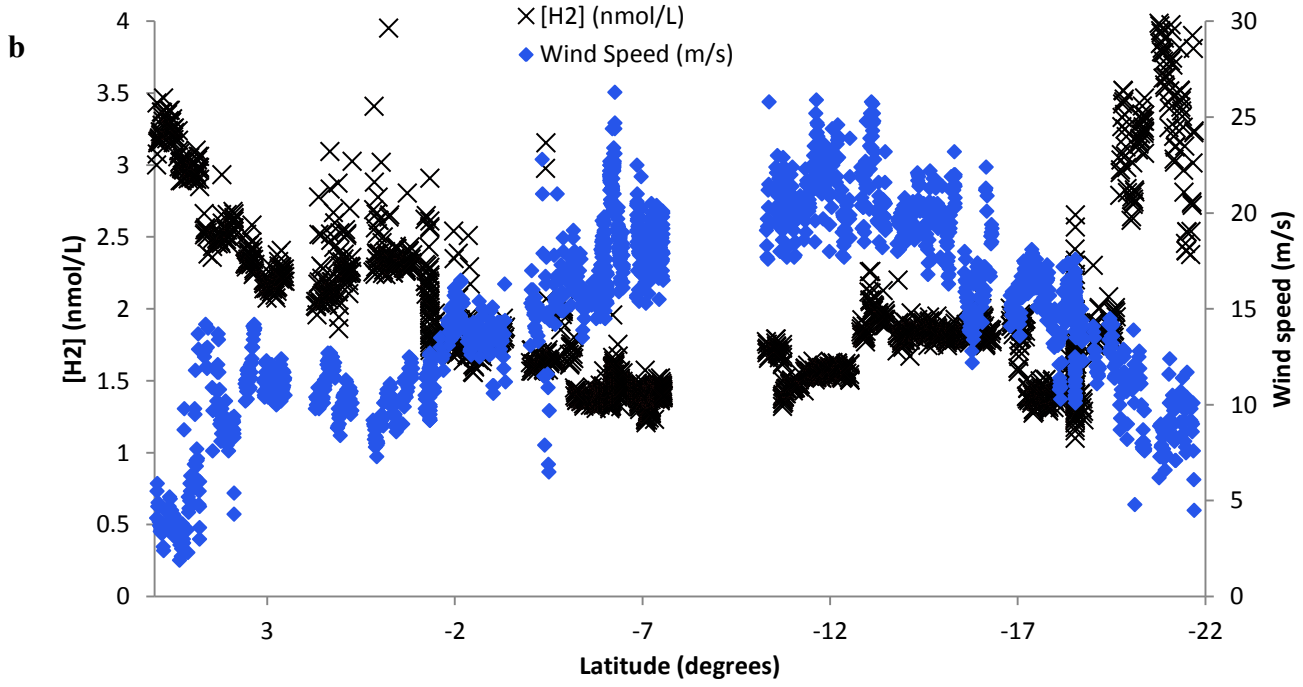

Figure 4.6b. Wind speed (m/s) and hydrogen concentrations measured between 6°N and 22°S

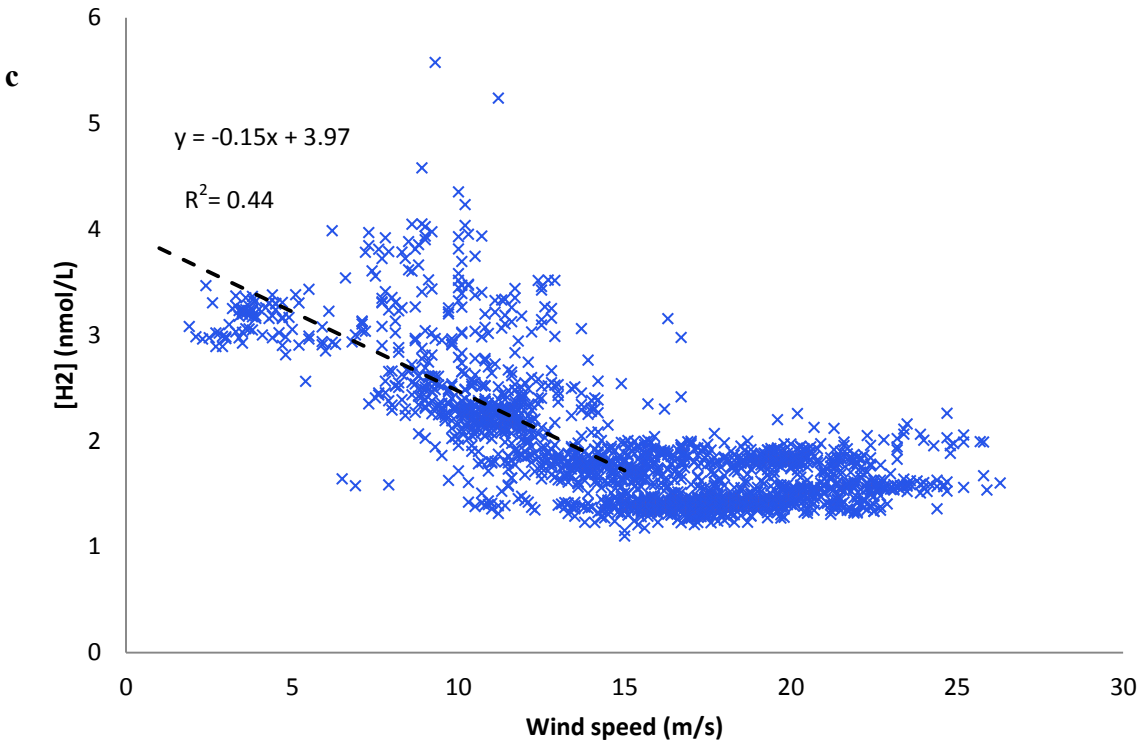

Figure 4.6c. Wind speed (m/s) plotted against hydrogen concentrations (nmol/L) measured between 6°N and 22°S with a linear regression for wind speeds less than 15m/s.

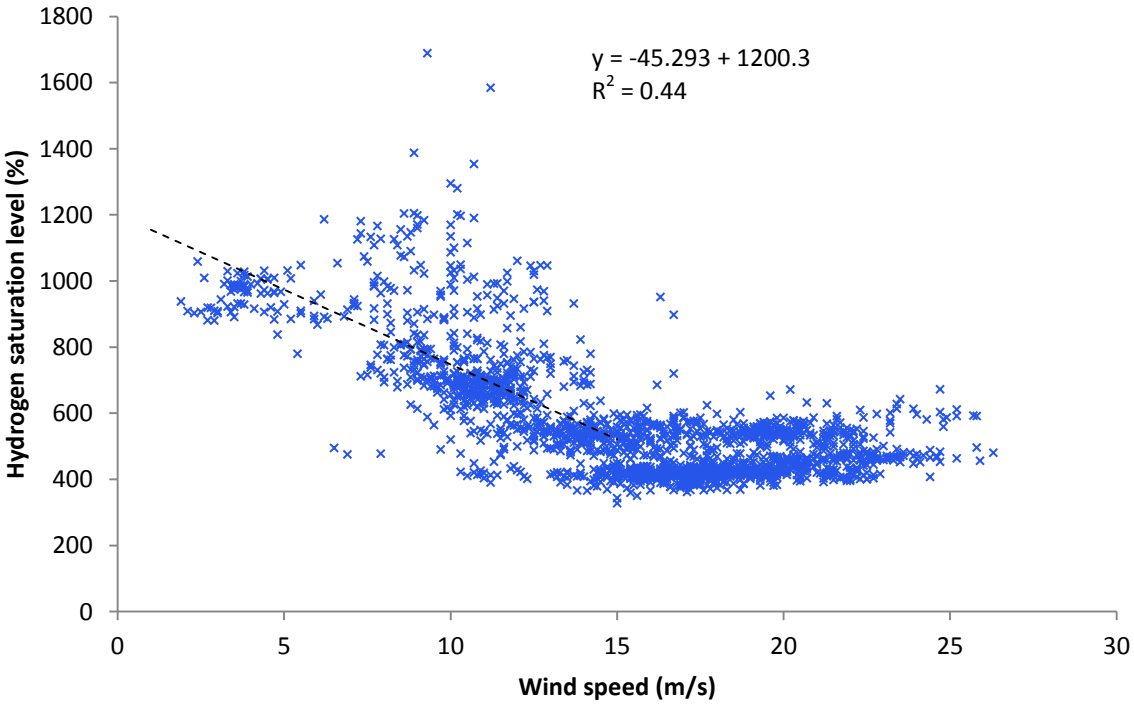

Figure 4.6d. Wind speed (m/s) plotted against hydrogen saturation level (%) measured between 6°N and 22°S with a linear regression for wind speeds less than 15m/s.

4.6 Sea surface temperature and hydrogen concentrations

Since sea surface temperature (SST) is important in determining the concentration at which oceanic H_2 is at equilibrium with the atmosphere, it might be expected that there would be some inverse correlation between the two parameters. There appear to be regions, however, where temperature and H_2 concentrations are positively correlated (figure 4.7). In one such region, between 5 and 50°N, SST and H_2 concentrations increase towards the equator. As previously suggested, the majority of nitrogen fixation in the North Atlantic is attributed to *Trichodesmium* (Moore, et al., 2009a) which is commonly found in waters with temperatures ranging from 20 to 34 °C (Breitbarth, Oschlies, & LaRoche, 2007). Therefore, elevated H_2 concentrations might be expected when we sample waters in this temperature range, but this is not observed in our study.

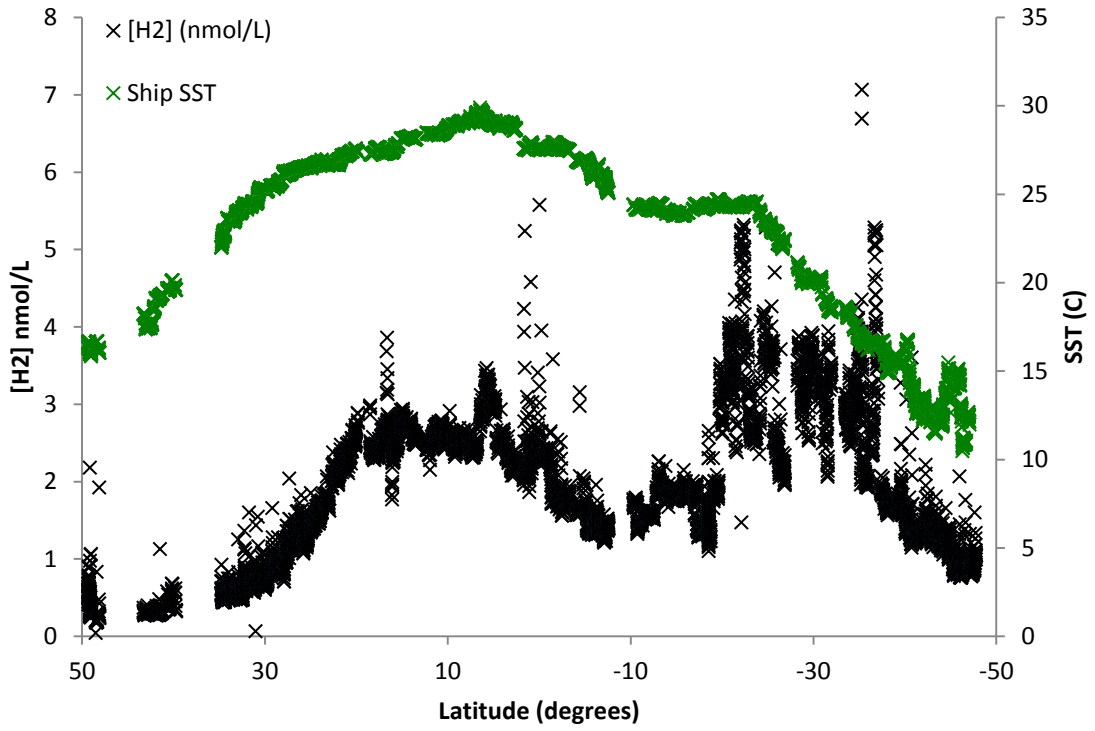

Figure 4.7. Sea surface temperature (°C) and hydrogen concentrations measured on AMT20.

4.7 Salinity and hydrogen concentrations

Although there is also a bimodal distribution of salinity along the AMT20 transect, there is little correlation with the distribution of H_2 concentrations (figure 4.8). The area with the lowest salinity, at ~10°N, is attributed to the influence of the Amazon River plume (Foster *et al.*, 2007). River plumes are known to supply iron and other nutrients to western tropical North Atlantic waters, which could potentially fuel nitrogen fixation. However, there is no change in H_2 concentration in the fresher river plume water. A spike in H_2 is observed at ~5°N however, when there is an increase in salinity, indicating a different water mass.

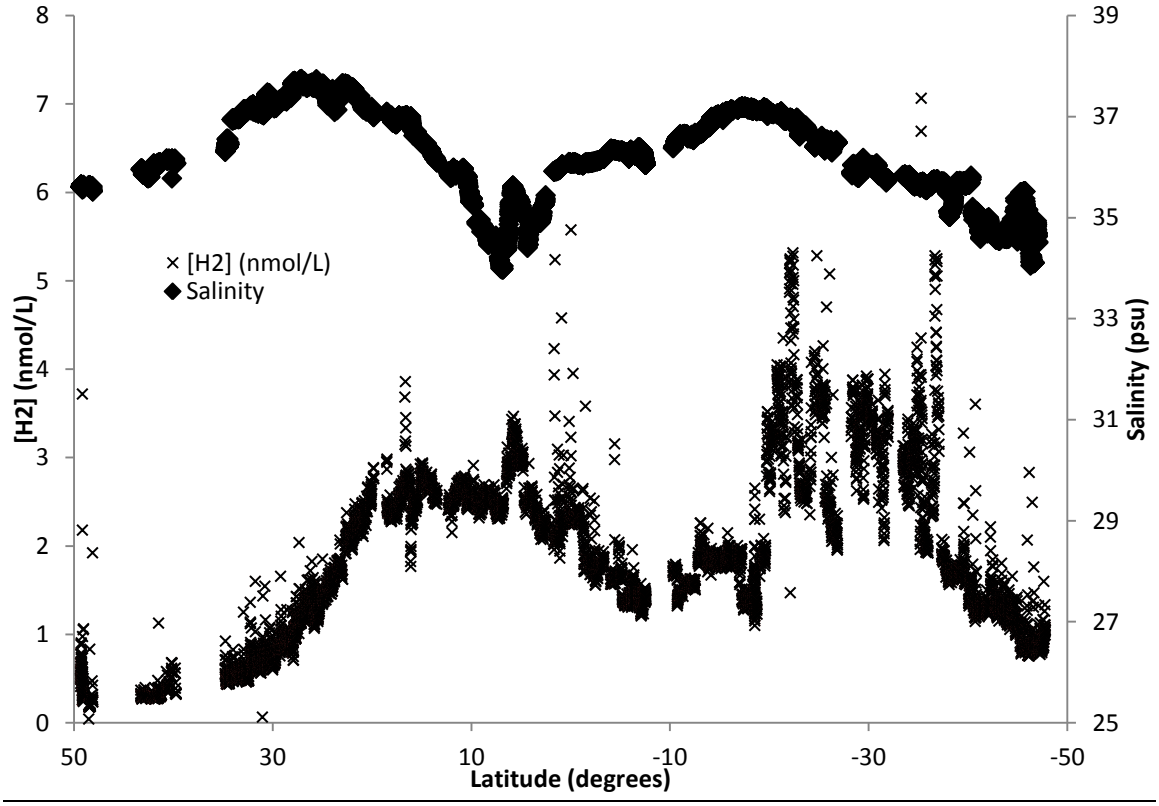

Figure 4.8. Salinity and hydrogen concentrations measured on AMT20.

4.8 Directions for future work

Major changes to the set up of the equilibrator would improve future work measuring H_2 concentrations. The equilibrator described in this thesis necessitates monitoring of many variables including temperature, gas and water flow rates and bubble patterns. The equilibrator was particularly sensitive to changes in water flow rate through the equilibrator coil, where changes ±1 mL/min can lead to an 8% change in the H_2 concentration. It would therefore be desirable to have a simpler equilibrator that was insensitive to changes in flow rates. Furthermore, because the equilibrator used in this study is prone to fouling (and sampling has to be stopped to clean it), the new equilibrator would ideally either be free from fouling or be easier to clean. The simpler design should also allow making H_2 measurements less labour intensive.

A major problem with making H_2 measurements is obtaining a water sample free from contamination. In future studies, having access to a tap that is close to the ship's water intake would be preferable, as any H_2 loss due to a biofilm in the ship's plumbing could be minimized. Collecting a water sample away from the research ship, perhaps from a non-metallic boat, would give an authentic H_2 concentration and would allow comparison between "clean" and potentially "contaminated" samples. Alternatively, a towed fish could be used to collect an uncontaminated sample. It would have to be deployed to the side of the ship to avoid the turbulence and contamination of the ship's wake. However, if suction was used to move the water sample from the towed fish to the ship, it would be expected to promote loss of dissolved gases into bubbles.

To provide further evidence of a link between H_2 concentrations and nitrogen fixation rates, many more simultaneous measurements of both parameters need to be made. Measurements of the *nif*H gene in conjunction with H_2 concentrations may also be useful in identifying which diazotrophs are contributing to the H_2 signal. Additionally, continuous measurements of iron concentrations,

which is thought to limit nitrogen fixation in some regions (Falkowski, 1997), would be of interest.

The negative correlation between wind speed and H_2 concentrations, from 6°N and 22°S, essentially coincides with the dip in the H_2 concentrations. Therefore it may be that the decrease in H_2 concentrations is due to the wind speed, rather than a decrease in nitrogen fixation. To estimate whether this is feasible, it will be necessary to calculate fluxes of H_2 from the mixed layer to the atmosphere and determine whether they are consistent with an approximately constant net production rate across this latitude range.

BIBLIOGRAPHY

Bothe, H., Schmitz, O., Yates, M., & Newton, W. (2011). Nitrogenases and hydrogenases in cyanobacteria. In G. A. Peschek, C. Obinger, & G. Regner, *Bioenergetic Processes of Cyanobacteria* (pp. 137-157). Dordrecht: Springer Netherlands.

Boyer, T., Antonov, J.I., Garcia, H., Johnson, D., Lacarnini, R., Mishonov, A., Smolyar, I. (2006). *World Ocean Atlas 2005.* Washington , D.C.: U.S. Government Printing Office.

Breitbarth, E., Oschlies, A., & LaRoche, J. (2007). Physiological constraints on the global distribution of *Trichodesmium* - effect of temperature on diazotrophy. *Biogeosciences*, 53-61.

Bullister, J. L., Jr, G., N.L, & Schink, D. R. (1982). Dissolved hydrogen, carbon monoxide, and Methane at the CEPEX site. *Journal of Geophysical Research*, 2022- 2034.

Burgess, B. K., & Lowe, D. J. (1996). Mechanism of molybdenum nitrogenase. *Chemistry Review, 96*, 2983-3011.

Constant, P., Poissant, L., & Villemur, R. (2009). Tropospheric H_2 budget and the response of its soil uptake under the changing environment. *Science of the Total Environment, 407*, 1809-1823.

Cullen, J. J. (1982). The deep chlorophyll maximum: comparing vertical profiles of chlorophyll *a*. *Can. J. Fish. Aquat. Sci.*, 791-803.

Deutsch, C., Sarmiento, J., Sigman, D., Gruber, N., & Dunne, J. (2007). Spatial coupling of nitrogen inputs and losses in the ocean. *Nature*, 163-167.

Dilworth, M. (1966). Acetylene reduction by nitrogen-fixing preparations from Clostridium pasteurum. *Biochimica et Biophysica Acta*, 285-294.

Falkowski, P. G. (1997). Evolution of the nitrogen cycle and its influence on the biological sequestration of CO_2 in the ocean. *Nature* , 272-275.

Foster, R., Subramaniam, A., Mahaffey, C., Carpenter, E., Capone, D., & Zehr, J. (2007). Influence of the Amazon River plume on distributions of free-living and symbiotic cyanbacteria in the western tropical North Atlantic. *Limnology and Oceanography*, 517-532.

Grosskopf, T., Mohr, W., Baustian, T., Schunck, H., Gill, D., Kuypers, M., . . . LaRoche, J. (in press). Doubling of marine N_2 fixation rates based on direct measurements.

Gruber, N., & Sarmiento, J. L. (1997). Global patterns of marine nitrogen fixation and denitrification. *Global Biogeochemical Cycles*, 1-33.

Herr, F., & Barger, W. (1978). Molecular hydrogen in the near-surface atmoshere and dissolved in waters in the tropical North Atlantic. *Journal of Geophysical Research, 83*(C12), 6199-6205.

Herr, F., Frank, E., Leone, G., & Kennicutt, M. (1984). Diurnal variability of dissolved molecular hydrogen in the tropical South Atlantic Ocean. *Deep-Sea Research, 31*(1), 13-20.

Herr, F., Scranton, M., & Barger, W. (1981). Dissolved hydrogen in the Norwegian Sea: Mesoscale surface variability and deep-water distribution. *Deep-Sea Research, 28A*(9), 1001-1016.

Hoffman, B., Dean, D., & Seefeldt, L. (2009). Climbing Nitrogenase: Toward a mechanism of enzymatic nitrogen fixation. *Accounts of Chemical Research, 42*(5), 609-619.

Holl, C. M., & Montoya, J. P. (2005). Interactions between nitrate uptake and nitrogen fixation in continuous cultures of *Trichodesmium* (cyanobacteria). *Journal of Phycology*, 1178-1183.

Hood, R., Coles, V., & Capone, D. (2004). Modeling the distribution of *Trichodesmium* and nitrogen fixation in the Atlantic Ocean. *Journal of Geophysical Research*, 1-25.

Karl, D., Letelier, R., Tupas, L., Dore, J., Christian, J., & Hebel, D. (1997). The role of nitrogen fixation in biogeochemical cycling in the North Pacific Ocean. *Nature* , 533-538.

Khalil, M., & Rasmussen, R. (1990). Global increase of atmospheric molecular hydrogen . *Nature* , 743-745.

Lavigne, H., Ortenzio, F., Claustre, H., & Poteau, A. (2012). Towards a merged satellite and in situ fluorescence ocean chlorophyll product. *Biogeoscience Discussions*, 11899-11939.

Mahaffey, C., Michaels, A. F., & Capone, D. G. (2005). The conundrum of marine N_2 fixation. *American Journal of Science, 305*, 546-595.

Mohr, W., Grosskopf, T., Wallace, D., & LaRoche, J. (2010). Methodological underestimation of oceanic nitrogen fixation rates. *PLoS ONE*, 1-7.

Moisander, P. H., Beinart, R. A., Hewson, I., White, A. E., Johnson, K. S., Carlson, C. A., Zehr, J. P. (2010). Unicellular cyanobacterial distributions broaden the oceanic N_2 fixation domain. *Science, 327*, 1512-1514.

Moore, C., Mills, M., Achterberg, E., Geider, R., LaRoche, J., Lucas, M., Woodward, E. M. (2009a). Large-scale distribution of Atlantic nitrogen fixation controlled by iron availability. *Nature Geoscience, 2*, 867-871.

Moore, R., Punshon, S., Mahaffey, C., & Karl, D. (2009). The relationship between dissolved hydrogen and nitrogen fixation in ocean waters. *Deep-Sea Research I*, 1449-1458.

Nagatani, H., Shimizu, M., & Valentine, R. (1971). The mechanism of ammonia assimilation in nitrogen fixing bacteria. *Arch. Mikrobiol*, 164-171.

Nandi, R., & Sengupta, S. (1998). Microbial production of hydrogen:An overview. *Critical Reviews in Microbiology*, 61-84.

Novelli, P., Lang, P., Masarie, K. A., Hurst, D., Myers, R., & Elkins, J. W. (1999). Molecular hydrogen in the troposphere: Global distribution and budget. *Journal of Geophysical Research, 104*, 30427-30444.

Ogo, S., Kure, B., Nakai, H., Watanabe, Y., & Fukuzumi, S. (2004). Why do nitrogenases waste electrons by evolving dihydrogen? *Applied Organometallic Chemistry, 18*, 589-594.

Punshon, S., & Moore, R. (2008a). Photochemical production of molecular hydrogen in lake water and coastal seawater. *Marine Chemistry*, 215-220.

Punshon, S., & Moore, R. (2008b). Aerobic hydrogen production and dinitrogen fixation in the marine cyanobacterium *Trichodesmium erythaeum* IMS101. *Limnology and Oceanography*, 2749-2753.

Punshon, S., Moore, R., & Xie, H. (2007). Net loss rates and distribution of molecular hydrogen (H_2) in mid latitude coastal waters. *Marine Chemistry*, 129-139.

Rivera-Ortiz, J., & Burris, R. (1975). Interactions among substrates and inhibitors of nitrogenase. *Journal of Bacteriology*, 537-545.

Schmidt, U. (1974). Molecular hydrogen in the atmosphere. *Tellus*, 78-90.

Scranton, M. (1984). Hydrogen cycling in the waters near Bermuda: the role of the nitrogen fixer, *Oscillatoria thiebautii*. *Deep-Sea Research, 31*, 133-143.

Scranton, M. I., & Brewer, P. (1977). Occurrence of methane in near-surface waters of the western subtropical North-Atlantic. *Deep Sea Research*, 127-138.

Scranton, M., Jones, M., & Herr, F. (1982). Distribution and variability of dissolved hydrogen in the Mediterranean Sea. *Journal of Marine Research, 40*(3), 873-891.

Scranton, M., Novelli, P., & Loud, P. (1984). The distribution and cycling of hydrogen gas in the waters of two anoxic marine environments. *Limnology and Oceanography, 29*(5), 993-1003.

Scranton, M., Novelli, P., Michaels, A., Horrigan, S., & Carpenter, E. (1987, July). Hydrogen production and nitrogen fixation by *Oscillitoria thiebautii* during in situ incubations. *Limnology and Oceanography, 32*(4), 998-1006.

Seiler, W., & Schmidt, U. (1974). Dissolved nonconservative gases in seawater. In E. Goldberg, *The Sea; ideas and observations on progress in the study of the seas.* (Vol. 5, pp. 219-243). New York: Wiley-Interscience.

Setser, P., Bullister, J., Frank, E., Guinasso Jr, N., & Schink, D. R. (1982). Relationships between reduced gases, nutrients, and fluorescence in surface waters off Baja California. *Deep-Sea Research*, 1203-1215.

Simmonds, P., Derwent, R., O'Doherty, S., Ryall, D., Steele, L., Langenfelds, R., Hudson, L. (2000). Continuous high-frequency observations of hydrogen at the Mace Head baseline atmospheric monitoring station over the 1994-1998 period. *Journal of Geophysical Research, 105*, 105-121.

Simpson, F. B., & Burris, R. H. (1984). A nitrogen pressure of 50 atmospheres does not prevent evolution of hydrogen by nitrogenase. . *Science*, 1095-1097 .

Team, R. D. (2012). *R: A language and environment for statistical.* Vienna, Austria: R Foundation for Statistical Computing.

Toepel, J., Welsh, E., Summerfield, T. C., Pakrasi, H. B., & Sherman, L. A. (2008). Differential transcriptional analysis of the cyanobacterium *Cyanothece sp*. strain ATCC 51142 during light-dark and continuous-light growth . *Journal of Bacteriology*, 3904- 3913.

Tukey, J. W. (1977). *Exploratory Data Analysis.* Reading: Addison-Wesley.

Tyrrell, T., Maranon, E., Poulton, A., Bowie, A., Harbour, D., & Woodward, E. (2003). Large-scale latitudinal distribution of *Trichodesmium spp*. in the Atlantic Ocean. *Journal of Plankton Research*, 405-416.

Uffen, R. (1978). Fermentative metabolism and growth of photosynthetic bacteria. In R. K. Clayton, & W. R. Sistrom, *The Photosynthetic Bacteria* (pp. 857-872). New York: Plenum.

Wiesenburg, D., & Guinasso, N. (1979). Equilibrium solubilities of methane, carbon monoxode and hydrogen in water and seawater. *Journal of Chemical and Engineering Data, 24*(4), 356-360.

Wilson, S., Foster, R., Zehr, J., & Karl, D. (2010a). Hydrogen production by *Trichodesmium erythaeum*, *Cyanothece sp*. and *Crocosphaera watsonii*. *Aquatic Microbial Ecology*, 197-206.

Wilson, S., Kolber, Z., Tozzi, S., Zehr, J. P., & Karl, D. M. (2012). Nitrogen fixation, hydrogen cycling and electron transport kinetics in *Trichodesmium erythraeum* (cyanobacteria) strain IMS101. *Phycological Society of America*, 1-12.

Wilson, S., Tozzi, S., Foster, R., Ilikchyan, I., Kolber, Z., Zehr, J., & Karl, D. (2010b йил October). Hydrogen cycling by the unicellular marine diazotroph *Crocosphaera watsonii* strain WH8501. *Applied and Environmental Microbiology, 76*(20), 6797-6803.

Wu, J., Sunda, W., Boyle, E. A., & Karl, D. M. (2000). Phosphate depletion in the western North Pacific Ocean. *Science*, 759-762.

Xie, H., Andrews, S., Martin, W., Miller, J., Ziolkowski, L., Taylor, C., & Zafiriou. (2002). Validated methods for sampling and headspace analysis of carbon monoxide in seawater. *Marine Chemistry*, 93-108.

Xie, H., Zafiriou, O. C., Wang, W., & Taylor, C. D. (2001). A simple automated continuous-flow-equilibration method for measuring carbon monoxide in seawater. *Environmental Science & Technology*, 1475-1480.

Zehr, J. (2011). Nitrogen fixation by marine cyanobacteria. *Trends in microbiology*, 162-173.

APPENDIX A

An example of a typical program to control the operation of the 4 solenoid valves that direct the flow of 3 gas streams; the sample, the low standard (1.135 ppm) and the zero air (air with very low H_2 concentrations). In this example, "rundata2.txt" is the name of the file the data will be saved to. "CYCLE" denotes which measurement of the run that the solenoid valves will be switched into the desired position."TIME" indicates the time during the cycle, when the valves will be switched to the position. Valve 1 (V1) controlled the flow (on/off) of the sample from the equilibrator and V2 controlled the flow of the zero air. V3 and V4 controlled the flow of the low standard.

rundata2.txt

CYCLE 0

TIME 5 SECONDS

V1 1

V2 0

V3 0

V4 0

CYCLE 18

TIME 5 SECONDS

V1 1

V2 0

V3 0

V4 1

CYCLE 20

TIME 5 SECONDS

V1 0

V2 0

V3 1

V4 1

CYCLE 24

TIME 5 SECONDS

V1 0

V2 1

V3 0

V4 0

CYCLE 28

TIME 5 SECONDS

V1 1

V2 0

V3 0

V4 0

CYCLE 46

TIME 5 SECONDS

V1 1

V2 0

V3 0

V4 1

CYCLE 48

TIME 5 SECONDS

V1 0

V2 0

V3 1

V4 1

CYCLE 52

TIME 5 SECONDS

V1 0

V2 1

V3 0

V4 0

CYCLE 56

TIME 5 SECONDS

APPENDIX B

R code used to identify the anomalous underway measurements using the running median function.

```
Hydrogen.data <- read.delim("C:/Users/Mike/Desktop/Hydrogen data.txt")
  View(Hydrogen.data)
 d <- read.delim("C:/Users/Mike/Desktop/Hydrogen data.txt", col.names=c("lat", "h2"))
 plot(d$lat, d$h2, xlab="latitude", ylab=expression(H[2]), cex=1/3)
 HH<- runmed(d$h2, k=11)
 deviation <- (d$h2 - HH) / sd(HH)
 cat("number of data:", length(d$h2), "\n")
 cat("chance of getting a point 3.6 SD above the mean is:", 1/(1-pnorm(3.6)), "\n")
 bad<- deviation > 3.6
 plot (d$lat[!bad], d$h2[!bad], xlab="Latitude (degrees)", ylab=expression(H[2] (nmol/L)),xlim=c(50, -50),
cex=1/3)
```

R code used to identify the anomalous underway measurements using the smooth function.

```
Hydrogen.data <- read.delim("C:/Users/Mike/Desktop/Hydrogen data.txt")
  View(Hydrogen.data)
 d <- read.delim("C:/Users/Mike/Desktop/Hydrogen data.txt", col.names=c("lat", "h2"))
 plot(d$lat, d$h2, xlab="latitude", ylab=expression(H[2]), cex=1/3)
HH <- smooth(d$h2)
 deviation <- (d$h2 - HH) / sd(HH)
 cat("number of data:", length(d$h2), "\n")
 cat("chance of getting a point 3.6 SD above the mean is:", 1/(1-pnorm(3.6)), "\n")
 bad<- deviation > 3.6
 plot (d$lat[!bad], d$h2[!bad], xlab="Latitude (degrees)", ylab=expression(H[2] (nmol/L)),xlim=c(50, -50),
cex=1/3)
```